Adiabatic expressions for the wave function of an electron in a finite-range potential and an intense low-frequency laser pulse

A. V. Flegel,[1] N. L. Manakov,[1] Ia. V. Breev,[1,2] and M. V. Frolov[1,2]
[1]*Department of Physics, Voronezh State University, Voronezh 394018, Russia*
[2]*Department of Radiophysics, University of Nizhny Novgorod, Nizhny Novgorod 603950, Russia*

(Received 18 June 2021; revised 12 August 2021; accepted 30 August 2021; published 15 September 2021)

The wave function of an electron interacting with a finite-range potential and an intense low-frequency laser pulse is analyzed within the adiabatic approximation. The closed analytic form for the wave function, which includes the rescattering corrections, is obtained with quasiclassical accuracy for an electron in both the initial bound and continuum states. We discuss the parametrizations of amplitudes of fundamental strong-field processes in terms of laser and binding-potential parameters. Based on the analytic results for the adiabatic wave functions, we develop the perturbation theory in an additional weak field. The modification of high-order harmonic generation amplitude caused by a weak extreme ultraviolet pulse is discussed in the first order of the perturbation theory.

DOI: 10.1103/PhysRevA.104.033109

I. INTRODUCTION

The quantum mechanical description of fundamental processes in an intense laser field consists in the calculation of corresponding transition matrix elements, which involve the exact wave function of an electron dynamically interacting with an intense laser field [1,2]. This wave function obeys the time-dependent Schrödinger equation (TDSE), whose solution for a given atomic potential and electron-laser interaction cannot be found in a closed analytic form. This obstacle can be overcome either by getting this wave function numerically from the TDSE [3,4] or by applying some approximations ensuring different levels of accuracy for the transition matrix element [1,5,6].

The mostly accepted approximation consists in the expansion of the wave function in the formal series in an atomic potential [1,5] (see also Refs. [7,8]). This expansion leads to the Born-like series for a transition amplitude, whose terms are associated with the n-times perturbative interaction of an electron with an atomic potential. These terms represent a partial amplitude of nth order in an atomic potential and can be expressed as a convolution of the Volkov Green's function with an atomic potential. Due to exponential dependence of the Volkov Green's function on the classical action of an electron in an intense low-frequency field, the partial amplitudes can be analyzed within the saddle-point method, resulting in the quantum orbit approach [9]. This approach provides a transparent physical interpretation of strong-field phenomena in terms of classical trajectories, and thereby it justifies the consistency of the rescattering model for fundamental processes in an intense laser field [1,5,10,11]. Moreover, the results obtained within the Born-like theory constitute a background for a parametrization of strong field processes amplitudes in terms of a product of laser and atomic parameters [12–15].

Although the approach based on the Born-like expansion has a big impact on the description of strong-field phenomena, it does not provide an accurate account of an atomic potential, whose influence on strong-field processes may be crucial [16–21]. In order to improve this issue, there were several attempts dealing with quasiclassical calculations of the exact quantum-mechanical propagator in an intense laser field [22,23] within the Feynman path-integral method [24,25]. In contrast to the Born-like formalism, in this approach an atomic potential enters the equation for quantum orbits (i.e., for calculations of classical trajectories with a complex initial condition). Although the mentioned approach shows reasonable agreement with numerical TDSE results for above-threshold ionization (ATI) spectra, there are open theoretical questions which require further discussions. For an intense low-frequency field, the part of classical action related to an atomic potential is significantly smaller than the part of action for a free electron in a laser field. Thus the seeming "exact" account of an atomic potential for a quantum orbit may lead to the exceeding accuracy in the calculated matrix element. Indeed, an atomic potential contributes more strongly to the slowly varying pre-exponential term, and it should be properly taken into account. Even in the case of comparable contribution to both the pre-exponential and exponential (through the classical action) factors, the influence of an atomic potential is considered only within the quasiclassical accuracy [26].

To the best of our knowledge, the first work in which the effects of an atomic potential were treated essentially exactly along with the quasiclassical accuracy for the account of electron-laser interaction is Ref. [27]. Based on the low-frequency (or adiabatic) approximation, Kroll and Watson [27] deduced the wave function of a continuum electron interacting with both an atomic potential and a laser field. The desired accuracy for the account of electron-laser interaction was restricted by the zero order in the ratio of electron-atom

scattering amplitude to the amplitude of the quiver motion of a free electron in a laser field. Within this accuracy, the laser-assisted scattering state is determined by the continuum state in atomic potential with modified asymptotic momentum, which is the kinematic electron momentum in a laser field. Although this result was intensively used for the calculation of collisional amplitudes [27,28], its extension for the treatment of rescattering-induced processes has not been yet discussed.

For an initially bound electron subjected to an intense laser field, the low-frequency approximation was suggested in Ref. [29]. In the lowest order of the low-frequency approximation, the shape of the wave function is given by the quasistationary state in the DC field [30], whose strength is determined by the instant strength of the laser electric field. The further development of the low-frequency approximation was focused mostly in two directions: (1) the decomposition in a series in frequency for the wave function [29] and (2) the development of an asymptotic solution of TDSE based on the solutions in the DC field [31]. In the latter case, the developed approach was successfully applied for description of plateau effects in spectra of the above-threshold detachment (ATD) [31] and high harmonic generation (HHG) [32].

There is no doubt that analytical approaches are in demand for deeper understanding of strong-field phenomena in terms of specific properties of the wave function in an intense laser field (see, e.g., Refs. [6,33]). The limited number of such analytical approaches stimulates us to extend in the present paper our recently developed adiabatic approach for the ATD analysis [34] to the description of the laser-dressed wave function. In particular, we focus our study on the "rescattering part" of the wave function for two cases, in which an electron is initially in either a bound or continuum state of a finite-range potential $U(r)$. In our analysis we take into account effects of the potential $U(r)$ essentially exactly, while effects of electron-laser interaction are treated with the quasiclassical accuracy. We show that the rescattering part of the wave function can be presented as a superposition of outgoing-wave scattering states with modified asymptotic momenta in the potential $U(r)$. Applying this result to the calculation of strong-field process amplitudes, we show that amplitude parametrizations are the result of specific properties of the wave function in an intense laser field. Moreover, we utilize the analytic results for the wave functions in an intense low-frequency laser field to develop the perturbation theory in some additional weak field. In particular, we apply this perturbation theory for calculation of corrections to the HHG amplitude caused by a weak attosecond pulse.

The paper is organized as follows: in Sec. II we give a short overview of the general equations for the wave function in an intense laser field; in Sec. III, within the low-frequency approximation, we discuss the wave function in an intense laser field for initially bound and continuum electrons; in Sec. IV we present practical applications of our analytical results for the wave function; in Sec. IV A we show the connection between parametrizations of strong-field process amplitudes and the analytical structure of the wave function; and in Sec. IV B the perturbation theory is developed with further application to the HHG in the presence of a weak extreme ultraviolet (XUV) pulse. A summary and outlook are given in Sec. V. All necessary mathematical details are given in Appendixes A and B. Atomic units (a.u.) are used throughout this paper unless specified otherwise.

II. GENERAL EQUATIONS

The study of strong field phenomena in the single active electron approximation is based on the TDSE solution:

$$i\frac{\partial\Psi(\boldsymbol{r},t)}{\partial t} = \hat{H}(\boldsymbol{r},t)\Psi(\boldsymbol{r},t),$$
$$\hat{H}(\boldsymbol{r},t) = \hat{T} + \hat{U}(\boldsymbol{r}) + \hat{V}(\boldsymbol{r},t), \quad (1)$$

where $\hat{T} = -\nabla^2/2$ is the kinetic energy operator, $\hat{U} = U(r)$ is the interaction potential of an active electron with an atomic target, and $\hat{V}(\boldsymbol{r},t)$ is the operator describing the electron-laser interaction. We consider the electron-laser interaction in the dipole approximation by applying the length gauge, which is the most appropriate for approximate estimations of the wave function and transition matrix elements [35–39]:

$$V(\boldsymbol{r},t) = \boldsymbol{r}\cdot\boldsymbol{F}(t),$$

where $\boldsymbol{F}(t)$ is the electric field of a laser pulse.

Equation (1) is accompanied by the initial condition formulated at some instant $t = t_0$ (the turning-on moment of the laser field):

$$\Psi(\boldsymbol{r},t)\big|_{t=t_0} = \Psi_0(\boldsymbol{r},t_0), \quad \Psi_0(\boldsymbol{r},t) = \varphi_0(\boldsymbol{r})e^{-iE_0t}, \quad (2)$$

where $\varphi_0(\boldsymbol{r})$ and E_0 are eigenstate and eigenvalue of the laser-field-free Hamiltonian $\hat{H}_0 = \hat{T} + \hat{U}$. [The state $\varphi_0(\boldsymbol{r})$ may be either discrete or continuum state of $\hat{H}_0$.] Formally, a solution of Eq. (1) can be written in terms of the nonstationary retarded Green's function, $\mathcal{G}(\boldsymbol{r},t;\boldsymbol{r}',t')$, for the Hamiltonian $\hat{H}(\boldsymbol{r},t)$ [36]:

$$\Psi(\boldsymbol{r},t) = \Psi_0(\boldsymbol{r},t) + \int_{-\infty}^{\infty}dt'\int d\boldsymbol{r}'\mathcal{G}(\boldsymbol{r},t;\boldsymbol{r}',t')V(\boldsymbol{r}',t')\Psi_0(\boldsymbol{r}',t'). \quad (3)$$

The Green's function satisfies the equation

$$\left[i\frac{\partial}{\partial t} - \hat{H}(\boldsymbol{r},t)\right]\mathcal{G}(\boldsymbol{r},t;\boldsymbol{r}',t') = \delta(\boldsymbol{r}-\boldsymbol{r}')\delta(t-t'), \quad (4)$$

and the condition $\mathcal{G}(\boldsymbol{r},t;\boldsymbol{r}',t') \equiv 0$ for $t < t'$.

It can be shown (see Appendix A) that the solution (3) for the case of a finite-range potential $U(r)$ satisfies the integral equation involving the retarded Volkov Green's function, $G_V(\boldsymbol{r},t;\boldsymbol{r}',t')$, for a free electron in a laser field:

$$\Psi(\boldsymbol{r},t) = \{\psi_{\boldsymbol{p}}^{(V)}(\boldsymbol{r},t)\} + \int_{-\infty}^{\infty}dt'\int d\boldsymbol{r}'G_V(\boldsymbol{r},t;\boldsymbol{r}',t')U(\boldsymbol{r}')\Psi(\boldsymbol{r}',t'), \quad (5)$$

where $\{\psi_{\boldsymbol{p}}^{(V)}(\boldsymbol{r},t)\} \equiv 0$ if the electron is initially in a bound state and $\{\psi_{\boldsymbol{p}}^{(V)}(\boldsymbol{r},t)\} \equiv \psi_{\boldsymbol{p}}^{(V)}(\boldsymbol{r},t)$ is the Volkov wave function if the electron initially is in a continuum spectrum. The retarded Green's function $G_V(\boldsymbol{r},t;\boldsymbol{r}',t')$ is a solution of the equation

$$\left[i\frac{\partial}{\partial t} - \hat{T} - \hat{V}(\boldsymbol{r},t)\right]G_V(\boldsymbol{r},t;\boldsymbol{r}',t') = \delta(\boldsymbol{r}-\boldsymbol{r}')\delta(t-t')$$

and has the form

$$G_V(\boldsymbol{r},t;\boldsymbol{r}',t') = -i\frac{\theta(t-t')}{(2\pi)^3}\int [\psi_{\boldsymbol{p}}^{(V)}(\boldsymbol{r}',t')]^*\psi_{\boldsymbol{p}}^{(V)}(\boldsymbol{r},t)\,d\boldsymbol{p}, \quad (6)$$

where $\theta(t-t')$ is the Heaviside step function,

$$\psi_{\boldsymbol{p}}^{(V)}(\boldsymbol{r},t) = e^{-i\phi_{\boldsymbol{p}}(t)+i\boldsymbol{P}(t)\cdot\boldsymbol{r}},$$
$$\boldsymbol{P}(t) = \boldsymbol{p}+\boldsymbol{A}(t), \quad \phi_{\boldsymbol{p}}(t) = \int^t \frac{\boldsymbol{P}^2(\tau)}{2}\,d\tau, \quad (7)$$

where $\boldsymbol{p}$ is the electron momentum and $\boldsymbol{A}(t)$ is the vector potential of a laser field with the electric vector $\boldsymbol{F}(t) = -d\boldsymbol{A}/dt$.

III. THE WAVE FUNCTION IN THE ADIABATIC LIMIT

An adiabatic analysis of the integral equation (5) was recently performed within the quasistationary quasienergy states approach [34]. Here we use a similar approach to obtain the explicit form for the wave function (3) in an intense low-frequency laser pulse, which evolves from an initial bound or continuum state $\Psi_0(\boldsymbol{r},t)$ of the Hamiltonian $\hat{H}_0$. The mathematical details of our derivations can be found in Appendix B, so we proceed in this section with final results and its discussion. We should note that an alternative approach for the analysis of the wave function in a strong laser field can be found also in Ref. [31].

A. The case of initial bound state

In the quasiclassical limit, the wave function (3) for the initially bound electron can be presented as the sum of the bound state $\varphi_0(\mathbf{r})$ with detachment threshold $I_p = -E_0$ and the rescattering part of the wave function, $\Phi^{(r)}(\boldsymbol{r},t)$, composed of the laser-field-free scattering states $\psi_{\boldsymbol{p}}^{(+)}(\boldsymbol{r})$ having the outgoing-wave asymptotics (see Appendix B)

$$\Psi(\boldsymbol{r},t) = e^{-iE_0t}[\varphi_0(\boldsymbol{r})+\Phi^{(r)}(\boldsymbol{r},t)], \quad (8a)$$
$$\Phi^{(r)}(\boldsymbol{r},t) = \sum_s a_s(t)\psi_{\boldsymbol{K}_s}^{(+)}(\boldsymbol{r}), \quad (8b)$$

where

$$a_s(t) = a_s^{(\mathrm{tun})}(t)a_s^{(\mathrm{pr})}(t), \quad (9a)$$
$$\boldsymbol{K}_s = \boldsymbol{k}_s+\boldsymbol{A}(t), \quad \boldsymbol{k}_s = -\frac{1}{t-t_s'}\int_{t_s'}^t \boldsymbol{A}(\tau)\,d\tau, \quad (9b)$$

and the index s enumerates the tunneling events happened at the time moments $t_s' \equiv t_s'(t)$. The tunneling time t_s' as a function of time t can be found from the (saddle-point) equation (see Ref. [40] for details)

$$\boldsymbol{K}_s'\cdot\dot{\boldsymbol{K}}_s' = 0, \quad (10)$$

where

$$\boldsymbol{K}_s' = \boldsymbol{k}_s+\boldsymbol{A}(t_s'), \quad \dot{\boldsymbol{K}}_s' = \frac{\partial \boldsymbol{K}_s'}{\partial t_s'}.$$

In Eq. (9a), the time-dependent "tunneling factor," $a_s^{(\mathrm{tun})}(t)$, is given by the tunneling exponent in the DC field of the strength $\mathcal{F}_s(t)$:

$$a_s^{(\mathrm{tun})}(t) \equiv a^{(\mathrm{tun})}(t,t_s') = C_{\kappa l}\frac{e^{-\frac{\varkappa_s^3(t)}{3\mathcal{F}_s(t)}}}{\sqrt{\varkappa_s(t)\mathcal{F}_s(t)}}Y_{lm}(\boldsymbol{e}_s), \quad (11)$$

where $C_{\kappa l}$ is the asymptotic coefficient of the bound state $\varphi_0(\boldsymbol{r})$:

$$\varphi_0(\boldsymbol{r})|_{\kappa r\gg 1} \approx C_{\kappa l}\frac{e^{-\kappa r}}{r}Y_{lm}(\hat{\boldsymbol{r}}), \quad \kappa = \sqrt{2I_p},$$

$Y_{lm}(\hat{\boldsymbol{r}})$ is the spherical harmonic, and

$$\varkappa_s(t) = \sqrt{\kappa^2+\boldsymbol{K}_s'^2}, \quad \mathcal{F}_s(t) = \sqrt{\boldsymbol{F}_s'^2-\boldsymbol{K}_s'\cdot\dot{\boldsymbol{F}}_s'},$$
$$\boldsymbol{F}_s' = \boldsymbol{F}(t_s'), \quad \dot{\boldsymbol{F}}_s' = \frac{\partial \boldsymbol{F}(t_s')}{\partial t_s'},$$
$$\boldsymbol{e}_s = (\boldsymbol{K}_s'+i\Delta_s\dot{\boldsymbol{K}}_s')/\kappa, \quad \Delta_s = \varkappa_s(t)/\mathcal{F}_s(t).$$

The propagation factor, $a_s^{(\mathrm{pr})}(t)$, is determined by the expression

$$a_s^{(\mathrm{pr})}(t) \equiv a^{(\mathrm{pr})}(t,t_s') = \frac{e^{iS(\boldsymbol{k}_s;t,t_s')}}{(t-t_s')^{3/2}}, \quad (12)$$
$$S(\boldsymbol{k}_s;t,t') = E_0(t-t')-\frac{1}{2}\int_{t'}^t [\boldsymbol{A}(\tau)+\boldsymbol{k}_s]^2 d\tau. \quad (13)$$

The general structure of $\Phi^{(r)}(\boldsymbol{r},t)$ shows that each partial term in sum (8b) is formed in two steps: the tunneling (the first step) creates a wave packet in the continuum, whose propagation (the second step) in the continuum leads to formation of the scattering state $\psi_{\boldsymbol{K}_s}^{(+)}(\boldsymbol{r})$ with the momentum $\boldsymbol{K}_s$. The contribution of different scattering states for a given time t is determined by the tunneling time t_s' and corresponding tunneling factor $a^{(\mathrm{tun})}(t,t_s')$. We should note that although the result (8) was obtained under the conditions of an "intense" laser field, $F^2/\omega^3 \gg 1$, and $I_p/\omega \gg 1$, there is also some additional restriction for the electric field strength, which justifies the appearance of a tunneling exponent (11) and the absence of any depletion factors in Eq. (9a): $F \ll F_{\mathrm{at}}$, where $F_{\mathrm{at}} = (2I_p)^{3/2}$ is a characteristic atomic field.

In Fig. 1 we present the time dependence of tunneling times t_s' for different laser pulses and use color coding to show the magnitude of tunneling factors. Our numerical examples show that the tunneling event is realized near the maximum of the electric field. In these examples we use pulses with linear [Fig. 1(a)] and elliptical [Fig. 1(b)] polarizations, two-color laser pulse with linearly polarized components in mutually perpendicular directions [Fig. 1(c)], and bicircular pulse [Fig. 1(d)]. All pulses are determined by the corresponding vector potentials:

$$\boldsymbol{A}_{\mathrm{a}}(t) = -\hat{\boldsymbol{x}}\frac{F}{\omega}f(t)\sin(\omega t), \quad (14a)$$
$$\boldsymbol{A}_{\mathrm{b}}(t) = -\frac{F}{\omega}f(t)\frac{\hat{\boldsymbol{x}}\sin(\omega t)-\eta\hat{\boldsymbol{y}}\cos(\omega t)}{\sqrt{1+\eta^2}}, \quad (14b)$$
$$\boldsymbol{A}_{\mathrm{c}}(t) = -\frac{F}{\omega}f(t)[\hat{\boldsymbol{x}}\sin(\omega t)-\hat{\boldsymbol{y}}\cos(2\omega t)], \quad (14c)$$
$$\boldsymbol{A}_{\mathrm{d}}(t) = -\frac{F}{\omega}f(t)\mathrm{Im}(\hat{\boldsymbol{e}}_+e^{-i\omega t}+\hat{\boldsymbol{e}}_-e^{-2i\omega t}), \quad (14d)$$

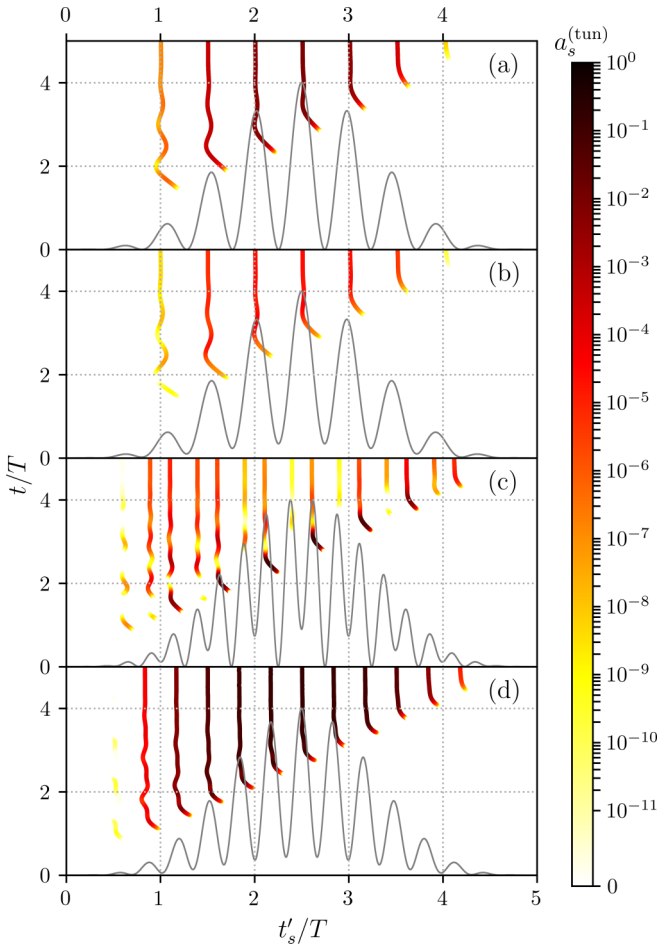

FIG. 1. The time dependence of roots of Eq. (10) $[t'_s(t)]$ for linearly polarized pulse (a), elliptically polarized pulse ($\eta = 0.3$) (b), two-color pulse with linearly polarized components in mutually perpendicular directions (c), and bicircular pulse (d). Thin gray lines show the time dependence of $F^2(t)$ (in arbitrary units). Color coding shows the magnitude of the tunneling factor (11) for the initial s-state ($l = m = 0$). $I = cF^2/(8\pi) = 10^{14}\,\mathrm{W/cm^2}$, $\hbar\omega = 0.62\,\mathrm{eV}$, $T = 2\pi/\omega$, c is the speed of light.

where F, ω, η are the strength, carrier frequency, and ellipticity of the field, $\hat{\boldsymbol{e}}_\pm = \mp(\hat{\boldsymbol{x}} \pm i\hat{\boldsymbol{y}})/\sqrt{2}$, and $f(t)$ is the $\sin^2$-envelope with the total duration $\mathcal{T} = 2\pi N/\omega$ with $N = 5$:

$$f(t) = \begin{cases} \sin^2\left(\frac{\pi t}{\mathcal{T}}\right) & t \in [0, \mathcal{T}] \\ 0 & \text{otherwise} \end{cases}.$$

B. The case of initial continuum state

For the scattering state of an electron with the asymptotic momentum $\boldsymbol{p}$ in an intense laser field, the wave function can be presented in the form (see Appendix B)

$$\Psi_{\boldsymbol{p}}(\boldsymbol{r}, t) = e^{-i\phi_{\boldsymbol{p}}(t)}\left[\psi^{(+)}_{\boldsymbol{P}(t)}(\boldsymbol{r}) + \Phi^{(r)}_{\boldsymbol{p}}(\boldsymbol{r}, t)\right], \tag{15a}$$

$$\Phi^{(r)}_{\boldsymbol{p}}(\boldsymbol{r}, t) = \sum_s A(\boldsymbol{K}'_s, \boldsymbol{P}'_s) a(\boldsymbol{p}; t, t'_s)\psi^{(+)}_{\boldsymbol{K}_s}(\boldsymbol{r}), \tag{15b}$$

where $A(\boldsymbol{K}'_s, \boldsymbol{P}'_s)$ is the amplitude of elastic electron scattering on the potential $U(r)$,

$$a(\boldsymbol{p}; t, t'_s) = \frac{e^{iS(\boldsymbol{p}, \boldsymbol{k}_s; t, t'_s)}}{\sqrt{\boldsymbol{F}'_s \cdot (\boldsymbol{p} - \boldsymbol{k}_s)(t - t'_s)^3}}, \tag{16a}$$

$$\boldsymbol{P}'_s \equiv \boldsymbol{P}(t'_s), \quad \boldsymbol{F}'_s = \boldsymbol{F}(t'_s). \tag{16b}$$

The times t'_s for this case are found from the equation

$$\boldsymbol{P}'^2_s = \boldsymbol{K}'^2_s. \tag{17}$$

We note that for possible complex solutions of Eq. (17) the vectors $\boldsymbol{P}'_s$ and $\boldsymbol{K}'_s$ are complex and the scattering amplitude is considered in the sense of analytic continuation for corresponding vectors.

The rescattering part of the wave function, $\Phi^{(r)}_{\boldsymbol{p}}(\boldsymbol{r}, t)$, in Eq. (15b) is presented as a linear combination of the scattering states, similarly to the case of a bound electron [see Eq. (8b)]. However, in contrast to the case of a bound electron, the formation of the scattering state with momentum $\boldsymbol{K}_s$ is realized through the scattering [determined by the scattering amplitude $A(\boldsymbol{K}'_s, \boldsymbol{P}'_s)$] and subsequent propagation [described by the factor $a(\boldsymbol{p}; t, t'_s)$]. Moreover, the coefficients at the laser-field-free scattering states in Eq. (15b) do not have exponential smallness, while they have smallness of the order $\sim|A|/a_q$ with respect to the plane wave term [see the first term in Eq. (15a)], where $|A|$ is the order of magnitude for the scattering amplitude, and $a_q = F/\omega^2$ is the quiver radius of free electron in a laser field [41,42]. We emphasize that $\Phi^{(r)}_{\boldsymbol{p}}(\boldsymbol{r}, t)$ gives a low-frequency correction to the well-known Kroll-Watson result [27]. In Fig. 2 we present the time dependence of t'_s for the same laser parameters as in Fig. 1 and electron momenta $\boldsymbol{p} = 1.2\hat{\boldsymbol{x}}$ and $\boldsymbol{p} = 1.2\hat{\boldsymbol{y}}$ a.u. In contrast to the case of an initial bound electron, the solutions $t'_s(t)$ of Eq. (17) depend on the momentum $\boldsymbol{p}$, which leads to more complex dependence on the laser pulse waveform. The collisional times t'_s require a special analysis for each particular geometry of the momentum $\boldsymbol{p}$ and vector potential $\boldsymbol{A}(t)$.

IV. DISCUSSION AND APPLICATIONS

In Sec. III, the time-dependent wave function in an intense laser field has been analyzed within the adiabatic approximation for an electron initially in a bound or continuum state. For these two cases the wave function can be partitioned into two, "slowly" and "rapidly" varying parts. For an initially bound electron, the slow part is given by the unperturbed initial state,[1] while for an initially free electron this part of the wave function is given by the laser-field-free scattering state with instantaneous momentum $\boldsymbol{P}(t)$ [see Eq. (15a)]. The rapidly varying parts for both cases are given by the linear combination of laser-field-free scattering states with different instantaneous momenta [cf. Eqs. (8b) and (15b)]. Since the amplitude of a strong-field process involves spatial and temporal integration of the function $\Psi(\boldsymbol{r}, t)$ [or $\Psi_{\boldsymbol{p}}(\boldsymbol{r}, t)$], the aforementioned representation of the rapidly varying part of

[1]The more accurate analysis of the integral equation (5) shows that this function should be replaced by the wave function in the static field with the instantaneous field strength $\boldsymbol{F}(t)$ [31].

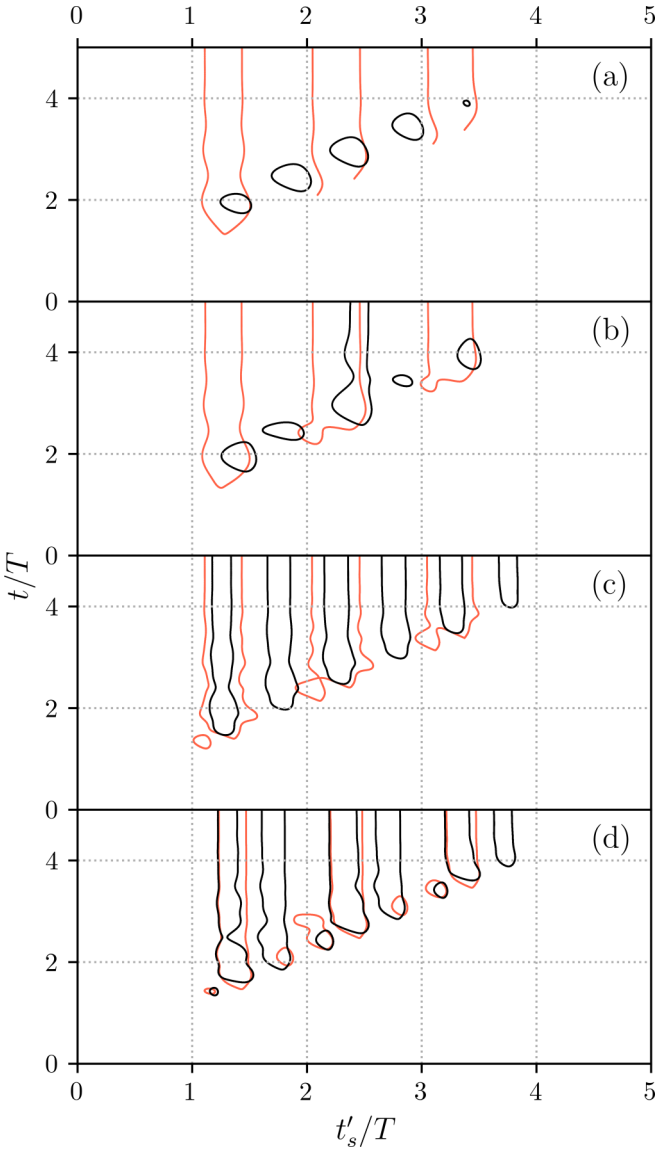

FIG. 2. The time dependence of roots of Eq. (17) $[t'_s(t)]$ for linearly polarized pulse (a), elliptically polarized pulse ($\eta = 0.3$) (b), two-color pulse with linearly polarized components in mutually perpendicular directions (c), bicircular pulse (d), and for two electron momenta: $\boldsymbol{p} = 1.2\hat{\boldsymbol{x}}$ a.u. (red lines), $\boldsymbol{p} = 1.2\hat{\boldsymbol{y}}$ a.u. (black lines). The laser parameters are the same as in Fig. 1.

$\Psi(\boldsymbol{r}, t)$ [or $\Psi_{\boldsymbol{p}}(\boldsymbol{r}, t)$] leads to the the specific form for the strong-field processes amplitudes, which describe reactions with the creations of high-energy electrons or photons. In particular, these amplitudes can be presented as a coherent sum of partial amplitudes, which are the product of a laser parameter and a laser-field-free amplitude of the photorecombination or the elastic electron scattering on an atomic core. Below in this section, we provide applications of our general results (8b) and (15b) for calculating the amplitudes of HHG, ATD for high-energy electrons, laser-assisted electron scattering (LAES), laser-assisted radiative attachment (LARA), and laser-assisted bremsstrahlung (LABrS).

Another application of the obtained results consists in analysis of the amplitudes of strong-field phenomena modified by a weak perturbation caused by an additional interaction with a field having different temporal or spatial properties. For instance, the interaction with the XUV field can be treated within the perturbation theory (see, e.g., Ref. [43]). In this section, we show how the results (8) and (15) can be effectively used for the development of the perturbation theory based on the nonperturbative wave functions of electron in the infrared (IR) field and the potential $U(r)$. For simplicity, we consider only the first order of the perturbation theory in a weak interaction and apply it to the HHG process.

A. Parametrization for amplitudes of fundamental processes in a strong laser field

1. High harmonic generation

The HHG process consists in the laser-stimulated photon emission with a frequency Ω and polarization vector $\boldsymbol{e}'_\Omega$. The HHG amplitude can be expressed in terms of the dipole transition matrix element [36]:

$$\mathcal{D}_{\rm HHG}(\Omega) = \int \langle \Psi_0(\boldsymbol{r}, t)|\boldsymbol{r}|\Psi^{(r)}(\boldsymbol{r}, t)\rangle e^{i\Omega t}\, dt, \tag{18}$$

where the function $\Psi^{(r)}(\boldsymbol{r}, t) = e^{-iE_0 t}\Phi^{(r)}(\boldsymbol{r}, t)$ and $\Phi^{(r)}(\boldsymbol{r}, t)$ is given by Eq. (8b). Substituting (8b) into Eq. (18) and integrating over t with methods suggested in Refs. [40,44], we obtain

$$\mathcal{D}_{\rm HHG}(\Omega) = \sum_j \mathcal{D}^{(j)}_{\rm HHG}(\Omega), \tag{19a}$$

$$\mathcal{D}^{(j)}_{\rm HHG}(\Omega) = e^{i\Omega t_j} a_j^{(\rm tun)} \overline{a}_j \boldsymbol{d}(\boldsymbol{K}_j), \tag{19b}$$

$$\overline{a}_j = \sqrt{\frac{2\pi i}{\boldsymbol{K}_j \cdot \boldsymbol{F}_j + \frac{\boldsymbol{K}_j^2}{t_j - t'_j}}}\, a_j^{(\rm pr)}, \quad \boldsymbol{F}_j = \boldsymbol{F}(t_j),$$

$$\boldsymbol{d}(\boldsymbol{K}_j) = \langle \varphi_0(\boldsymbol{r})|\boldsymbol{r}|\psi^{(+)}_{\boldsymbol{K}_j}(\boldsymbol{r})\rangle, \tag{19c}$$

where $a_j^{(\rm tun)} \equiv a^{(\rm tun)}(t_j, t'_j)$ and $a_j^{(\rm pr)} \equiv a^{(\rm pr)}(t_j, t'_j)$ are tunneling [see Eq. (11)] and propagation [see Eq. (12)] factors, calculated for the jth pair of tunneling (t'_j) and recombination (t_j) times (for details, see Refs. [40,44]). The values of times t'_j and t_j are found from the coupled system of two transcendental equations:

$$\boldsymbol{K}'_j \cdot \dot{\boldsymbol{K}}'_j = 0, \quad \boldsymbol{K}'^2_j = 2(\Omega + E_0), \tag{20}$$

where

$$\boldsymbol{K}'_j = \boldsymbol{A}(t'_j) - \frac{1}{t_j - t'_j}\int_{t'_j}^{t_j} \boldsymbol{A}(\tau)\, d\tau, \quad \dot{\boldsymbol{K}}'_j = \frac{\partial \boldsymbol{K}'_j}{\partial t'_j},$$

$$\boldsymbol{K}_j = \boldsymbol{A}(t_j) - \frac{1}{t_j - t'_j}\int_{t'_j}^{t_j} \boldsymbol{A}(\tau)\, d\tau.$$

Using the obtained expression (19a) for the HHG amplitude, the HHG yield (summed over photon polarizations), $\mathcal{Y}_{\rm HHG}$, can be presented in the well-known factorized form [45]

$$\mathcal{Y}_{\rm HHG} = \frac{|\mathcal{D}_{\rm HHG}(\Omega)|^2}{4\pi^2 c^3} = W(E)\sigma_{\rm rec}, \tag{21}$$

where $W(E)$ is the electron wave packet and $\sigma_{\rm rec}$ is the exact photorecombination cross section for the potential $U(r)$.

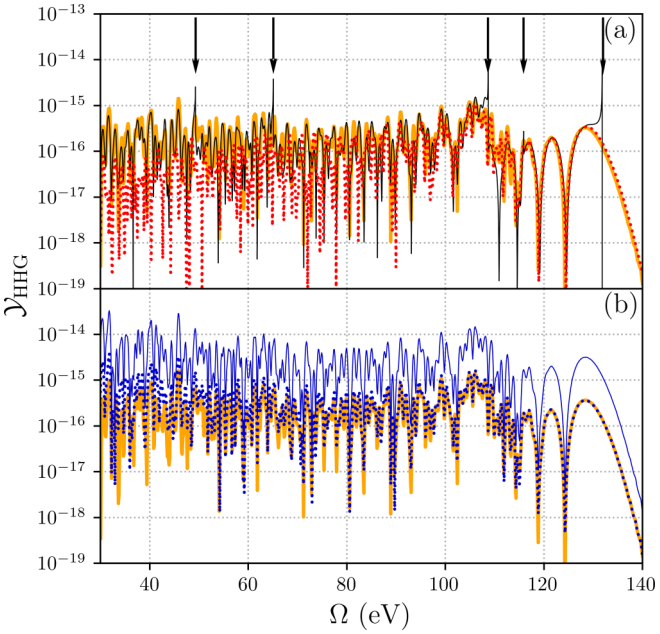

FIG. 3. (a) HHG yield (21) for the potential (22) ($U_0 = 1.908$, $\alpha = 1$) and linearly polarized pulse with parameters as in Fig. 1(a). Solid thick orange line: the result extracted from the numerical TDSE solution; thin black line: the result obtained with analytical expression (19); red dotted line: the analytical result from Ref. [44]. Arrows show positions of merging of short and long classical electron trajectories. (b) Numerical TDSE results for HHG spectra for the potential (22) and linearly polarized pulse with laser parameters as in Fig. 1(a). Solid thick orange line is the same as in panel (a) ($U_0 = 1.908, \alpha = 1$); blue thin line: the result for $U_0 = 1.1, \alpha = 0.1$; dotted blue line: the scaled result for $U_0 = 1.1$, $\alpha = 0.1$ (the scaling factor is 0.114).

In Fig. 3(a) we present a comparison of the analytical result (19) with corresponding result obtained from the numerical solution of the TDSE for the Yukawa potential:

$$U(r) = -U_0 \frac{e^{-\alpha r}}{r}. \tag{22}$$

Calculations were performed for $U_0 = 1.908$, $\alpha = 1$, and linearly polarized pulse (14a) (with peak intensity 10^{14} W/cm^2, $N = 5$, and carrier frequency $\hbar\omega = 0.62$ eV) using the algorithm described in Refs. [40,44]. The analytical result (19) is in a good agreement with the TDSE result excluding narrow vicinities of the zeros of second derivative of the action (13), which corresponds to merging of short and long electron trajectories [see arrows in Fig. 3(a)]. In these areas the HHG amplitude can be treated more precisely (in terms of the Airy function) in order to remove the unphysical peaks in HHG spectra (see Ref. [44]).

In Fig. 3(b) we compare high-energy parts of HHG spectra calculated for two different parameters of the potential (22): $U_0 = 1.908$, $\alpha = 1$ and $U_0 = 1.1$, $\alpha = 0.1$. For the first set of parameters, the potential (22) supports a single bound state with binging energy $E_{1s} = -13.6$ eV, while for the second set there are two bound states with $E_{1s} = -13.6$ eV and $E_{2s} = -1.8$ eV. Our results show that key scaled parameters for the high-energy harmonic yield are the binding energy and the asymptotic coefficient in the wave function of an initial state, as well as the intensity and carrier frequency of laser pulse. If these parameters are the same for two cases, the shape of the high-energy parts of HHG spectra is similar.

2. Above-threshold detachment

Laser-induced ionization or detachment of an atomic system accompanies any process in an intense laser field by creating electrons in the continuum. The energies of these electrons may exceed the characteristic energy of a free electron in a laser field, which is $u_p = F^2/(4\omega^2)$. The corresponding transition amplitude for producing such fast electrons is expressed in terms of the function $\Psi^{(r)}(\boldsymbol{r}, t)$ [34]:

$$\mathcal{A}^{(r)}_{\rm ATD}(\boldsymbol{q}) = -\frac{1}{4\pi^2}\int \langle \psi^{(V)}_{\boldsymbol{q}}(\boldsymbol{r}, t)|U(r)|\Psi^{(r)}(\boldsymbol{r}, t)\rangle\, dt, \tag{23}$$

where $\boldsymbol{q}$ is the momentum of an ionized electron. Substituting the explicit form of the Volkov wave function and $\Phi^{(r)}(\boldsymbol{r}, t)$ [see Eqs. (7) and (8b), respectively], taking into account the definition for T-matrix (B7), and integrating in Eq. (23) over t by the saddle-point method (see details in Ref. [34]), we obtain

$$\mathcal{A}^{(r)}_{\rm ATD}(\boldsymbol{q}) = \sum_j \mathcal{A}^{(r)}_{{\rm ATD},j}(\boldsymbol{q}), \tag{24a}$$

$$\mathcal{A}^{(r)}_{{\rm ATD},j}(\boldsymbol{q}) = e^{i[\phi_{\boldsymbol{q}}(t_j) - E_0 t_j]} a^{(\rm tun)}_j \check{a}_j A(\boldsymbol{Q}_j, \boldsymbol{K}_j),$$

$$\check{a}_j = \sqrt{\frac{2\pi i}{(\boldsymbol{K}_j - \boldsymbol{Q}_j)\cdot \boldsymbol{F}_j + \frac{\boldsymbol{K}_j^2}{t_j - t'_j}}}\, a^{(\rm pr)}_j,$$

$$\boldsymbol{Q}_j = \boldsymbol{q} + \boldsymbol{A}(t_j), \tag{24b}$$

where $a^{(\rm tun)}_j$ and $a^{(\rm pr)}_j$ are given by Eqs. (11) and (12) for the jth tunneling and rescattering events corresponding to time instants t'_j and t_j. The details of calculation of real tunneling and rescattering times t'_j and t_j can be found in Refs. [34,46]. For high-energy electrons, the differential detachment yield is given by

$$dW = 2\pi q |\mathcal{A}^{(r)}_{\rm ATD}(\boldsymbol{q})|^2\, dE_q\, d\Omega_{\boldsymbol{q}}, \tag{25}$$

where $E_q = q^2/2$ and $d\Omega_{\boldsymbol{q}}$ is the solid angle along the momentum $\boldsymbol{q}$. We note that the good agreement of the analytical result (24) with the result extracted from the numerical solution of the TDSE for the Yukawa potential has been demonstrated in Ref. [34].

3. Laser-assisted electron scattering

An incident electron can be elastically scattered on atomic target in the presence of an intense laser pulse with changing its momentum and energy due to interaction with a laser field. The amplitude of such an LAES process can be expressed in terms of the Volkov wave function and exact continuum state in a laser field (see, e.g., Ref. [27]):

$$\mathcal{A}_{\rm LAES}(\boldsymbol{q}, \boldsymbol{p}) = -\frac{1}{4\pi^2}\int \langle \psi^{(V)}_{\boldsymbol{q}}(\boldsymbol{r}, t)|U(r)|\Psi_{\boldsymbol{p}}(\boldsymbol{r}, t)\rangle\, dt, \tag{26}$$

where $\boldsymbol{p}$ and $\boldsymbol{q}$ are initial and final momenta of the electron. For a given LAES amplitude, the differential scattering cross

section is

$$d\sigma = \frac{q}{p}|\mathcal{A}_{\rm LAES}(\boldsymbol{q},\boldsymbol{p})|^2 dE_q\, d\Omega_{\boldsymbol{q}}. \tag{27}$$

The LAES amplitude can be partitioned into two terms, according to the two-term expression (B26)

$$\mathcal{A}_{\rm LAES}(\boldsymbol{q},\boldsymbol{p}) = \mathcal{A}^{(s)}_{\rm LAES}(\boldsymbol{q},\boldsymbol{p}) + \mathcal{A}^{(r)}_{\rm LAES}(\boldsymbol{q},\boldsymbol{p}),$$

where the first term, $\mathcal{A}^{(s)}_{\rm LAES}(\boldsymbol{q},\boldsymbol{p})$, corresponds to the first term in expression (15a), while the second term, $\mathcal{A}^{(r)}_{\rm LAES}(\boldsymbol{q},\boldsymbol{p})$, is determined by $\Phi^{(r)}_{\boldsymbol{p}}(\boldsymbol{r},t)$. The spatial integration in these two amplitudes is performed using the definition of a T-matrix (B7), while the integration over the time t by the saddle-point method shows that obtained T-matrices are taken on the energy shell and can be replaced by amplitudes of elastic scattering [see Eq. (B25)]. Routine calculations give for $\mathcal{A}^{(s)}_{\rm LAES}(\boldsymbol{q},\boldsymbol{p})$

$$\mathcal{A}^{(s)}_{\rm LAES}(\boldsymbol{q},\boldsymbol{p}) = \sum_j \mathcal{A}^{(s)}_{{\rm LAES},j}(\boldsymbol{q},\boldsymbol{p}), \tag{28a}$$

$$\mathcal{A}^{(s)}_{{\rm LAES},j} = a^{(s)}_j(\boldsymbol{q},\boldsymbol{p}) A(\boldsymbol{Q}_j,\boldsymbol{P}_j), \tag{28b}$$

$$a^{(s)}_j(\boldsymbol{q},\boldsymbol{p}) = \sqrt{\frac{2\pi i}{\boldsymbol{F}_j\cdot(\boldsymbol{p}-\boldsymbol{q})}}\, e^{i[\phi_{\boldsymbol{q}}(t_j)-\phi_{\boldsymbol{p}}(t_j)]},$$

$$\boldsymbol{P}_j = \boldsymbol{p} + \boldsymbol{A}(t_j), \tag{28c}$$

where $a^{(s)}_j(\boldsymbol{q},\boldsymbol{p})$ is the laser factor and t_j is the solution of transcendental (saddle-point) equation

$$\boldsymbol{Q}_j^2 = \boldsymbol{P}_j^2. \tag{29}$$

For the monochromatic linearly polarized field, the factor $A(\boldsymbol{Q}_j,\boldsymbol{P}_j)$ does not depend on the index j and can be factored out [42]. For this case the scattering cross section [corresponding to the amplitude $\mathcal{A}^{(s)}_{\rm LAES}(\boldsymbol{q},\boldsymbol{p})$] can be presented as the product of the laser factor (expressed in terms of the Bessel function) and exact elastic electron scattering cross section on the potential $U(r)$ [27]. For arbitrary laser field shape, the direction and length of the vector $\boldsymbol{Q}_j$ depend on j (see, e.g., Ref. [42]), and factorization of the scattering cross section on laser factor and field-free cross section is impossible.

Similar calculations give the expression for amplitude $\mathcal{A}^{(r)}_{\rm LAES}(\boldsymbol{p},\boldsymbol{q})$, which describes high-energy or rescattering electrons [42]:

$$\mathcal{A}^{(r)}_{\rm LAES}(\boldsymbol{q},\boldsymbol{p}) = \sum_j \mathcal{A}^{(r)}_{{\rm LAES},j}, \tag{30a}$$

$$\mathcal{A}^{(r)}_{{\rm LAES},j} = A(\boldsymbol{K}'_j,\boldsymbol{P}'_j)\tilde{a}(\boldsymbol{p};t_j,t'_j)A(\boldsymbol{Q}_j,\boldsymbol{K}_j), \tag{30b}$$

$$\tilde{a}(\boldsymbol{p};t_j,t'_j) = \sqrt{\frac{2\pi i}{\boldsymbol{F}_j\cdot(\boldsymbol{k}_j-\boldsymbol{q})}} \times a(\boldsymbol{p};t_j,t'_j) e^{i[\phi_{\boldsymbol{q}}(t_j)-\phi_{\boldsymbol{p}}(t_j)]},$$

$$\boldsymbol{P}'_j = \boldsymbol{p} + \boldsymbol{A}(t'_j), \tag{30c}$$

where $a(\boldsymbol{p};t_j,t'_j)$ is given by Eq. (16a) and pair of times t_j, t'_j is the solution of the system of saddle-point equations:

$$\boldsymbol{P}'^{\,2}_j = \boldsymbol{K}'^{\,2}_j, \quad \boldsymbol{K}_j^2 = \boldsymbol{Q}_j^2. \tag{31}$$

4. Laser-assisted radiative attachment

An electron being in the continuum may spontaneously emit a photon passing into a bound state. This process can be assisted by a laser field, which induces new channels for the radiative recombination or attachment. The LARA amplitude is expressed in terms of the functions $\Psi(\boldsymbol{r},t)$ and $\Psi_p(\boldsymbol{r},t)$:

$$\mathcal{D}_{\rm LARA}(\Omega) = \int \langle\tilde{\Psi}(\boldsymbol{r},t)|\boldsymbol{r}|\Psi_{\boldsymbol{p}}(\boldsymbol{r},t)\rangle e^{i\Omega t}\, dt, \tag{32}$$

where Ω is the frequency of spontaneous photon, and $\tilde{\Psi}(\boldsymbol{r},t) = e^{-iE_0 t}\tilde{\Phi}(\boldsymbol{r},t)$ is the dual function with the asymptotics of ingoing spherical waves at large distances [47–49]. The dual function can be obtained from $\Psi(\boldsymbol{r},t)$ by complex conjugation, reversing the time and all time-odd quantities. However, $\tilde{\Psi}(\boldsymbol{r},t)$ may be approximated by $\Psi_0(\boldsymbol{r},t) = e^{-iE_0 t}\varphi_0(\boldsymbol{r})$ since the rescattering part has the exponential smallness [caused by the tunneling factor (11)]. The LARA cross section (integrated over directions and summed over polarizations of the emitted photon) is given by

$$d\sigma = \frac{\Omega^3|\mathcal{D}_{\rm LARA}(\Omega)|^2}{3\pi^2 c^3 p\mathcal{T}}\, d\Omega, \tag{33}$$

where $\mathcal{T}$ is the duration of a laser pulse.[2]

Substituting the two-terms result (15a) for $\Psi_{\boldsymbol{p}}(\boldsymbol{r},t)$ into Eq. (32) and approximating $\tilde{\Psi}(\boldsymbol{r},t)$ by $\Psi_0(\boldsymbol{r},t)$, the amplitude (32) in the adiabatic limit reduces to

$$\mathcal{D}_{\rm LARA}(\Omega) = \mathcal{D}^{(s)}_{\rm LARA}(\Omega) + \mathcal{D}^{(r)}_{\rm LARA}(\Omega). \tag{34}$$

The expression for $\mathcal{D}^{(s)}_{\rm LARA}(\Omega)$ is

$$\mathcal{D}^{(s)}_{\rm LARA}(\Omega) = \sum_j \hat{a}^{(s)}_j \boldsymbol{d}(\boldsymbol{P}_j), \tag{35a}$$

$$\hat{a}^{(s)}_j = \sqrt{\frac{2\pi i}{\boldsymbol{F}_j\cdot\boldsymbol{P}_j}}\, e^{i[(\Omega-I_p)t_j-\phi_{\boldsymbol{p}}(t_j)]}, \tag{35b}$$

where $\boldsymbol{d}(\boldsymbol{P}_j)$ is given by Eq. (19c) replacing $\boldsymbol{K}_j \to \boldsymbol{P}_j$. [For linearly polarized monochromatic field, as for the case of LAES, $\boldsymbol{d}(\boldsymbol{P}_j)$ can be factored out.] The time t_j satisfies the equation

$$\boldsymbol{P}_j^2 = 2(\Omega - I_p).$$

The similar consideration gives the result for the rescattering part of the LARA amplitude $\mathcal{D}^{(r)}_{\rm LARA}(\Omega)$:

$$\mathcal{D}^{(r)}_{\rm LARA}(\Omega) = \sum_j \mathcal{D}^{(r)}_{{\rm LARA},j}(\Omega), \tag{36a}$$

$$\mathcal{D}^{(r)}_{{\rm LARA},j}(\Omega) = e^{i\Omega t_j} A(\boldsymbol{K}'_j,\boldsymbol{P}'_j)\hat{a}(\boldsymbol{p};t_j,t'_j)\boldsymbol{d}_j, \tag{36b}$$

$$\hat{a}(\boldsymbol{p};t_j,t'_j) = \sqrt{\frac{2\pi i}{\boldsymbol{F}_j\cdot\boldsymbol{K}_j}}\, a(\boldsymbol{p};t_j,t'_j) e^{i[E_0 t_j-\phi_{\boldsymbol{q}}(t_j)]}, \tag{36c}$$

where $\boldsymbol{d}_j$ is determined by Eq. (19c) and the pair of times $\{t'_j,t_j\}$ is found from the coupled system of Eqs. (B23) and (20):

$$\boldsymbol{P}'^{\,2}_j = \boldsymbol{K}'^{\,2}_j, \quad \boldsymbol{K}_j^2 = 2(\Omega - I_p). \tag{37}$$

[2]Note that $d\sigma/d\Omega$ tends to zero at $\mathcal{T}\to 0$, since $\mathcal{D}_{\rm LARA}(\Omega)\propto\mathcal{T}$ in this case.

5. Laser-assisted bremsstrahlung

The LABrS is the fundamental process in an intense laser field, in which an electron emits the spontaneous photon being in the continuum. For the initial and final electron momenta $\boldsymbol{p}$ and $\boldsymbol{q}$, the LABrS amplitude is given by the expression [28]

$$\mathcal{D}_{\rm BrS}(\boldsymbol{q},\boldsymbol{p};\Omega)=\int\langle\tilde{\Psi}_{\boldsymbol{q}}(\boldsymbol{r},t)|\boldsymbol{r}|\Psi_{\boldsymbol{p}}(\boldsymbol{r},t)\rangle e^{i\Omega t}\,dt, \tag{38}$$

where Ω is the frequency of spontaneous photon, and $\tilde{\Psi}_{\boldsymbol{q}}(\boldsymbol{r},t)$ is the continuum state, whose asymptotics at large distances contains the Volkov state and ingoing spherical waves. This wave function can be obtained from the function $\Psi_{\boldsymbol{q}}(\boldsymbol{r},t)$ [cf. Eq. (15a)] as follows (see, e.g., Ref. [50]):

$$\tilde{\Psi}_{\boldsymbol{q}}(\boldsymbol{r},t)=\Psi^{*}_{-\boldsymbol{q}}(\boldsymbol{r},-t)\Big|_{\boldsymbol{A}(t)\to-\boldsymbol{A}(-t)}. \tag{39}$$

The LABrS cross section $d\sigma/d\Omega$ with emission of the spontaneous photon of energy Ω (integrated over directions and summed over polarizations of the photon) is given by

$$\frac{d\sigma}{d\Omega}=\int\frac{2\Omega^3|\mathcal{D}_{\rm BrS}(\boldsymbol{q},\boldsymbol{p};\Omega)|^2}{3c^3\pi^3 p\mathcal{T}}\frac{d\boldsymbol{q}}{(2\pi)^3}. \tag{40}$$

The dipole matrix element $\mathcal{D}_{\rm BrS}(\boldsymbol{q},\boldsymbol{p};\Omega)$ can be partitioned into two parts:

$$\mathcal{D}_{\rm BrS}(\boldsymbol{q},\boldsymbol{p};\Omega)=\mathcal{D}^{(s)}_{\rm BrS}(\boldsymbol{q},\boldsymbol{p};\Omega)+\mathcal{D}^{(r)}_{\rm BrS}(\boldsymbol{q},\boldsymbol{p};\Omega). \tag{41}$$

The first part corresponds to the transition between two laser-field-free scattering states in the potential $U(r)$:

$$\mathcal{D}^{(s)}_{\rm BrS}(\boldsymbol{q},\boldsymbol{p};\Omega)=\int e^{i[\phi_{\boldsymbol{q}}(t)-\phi_{\boldsymbol{p}}(t)+\Omega t]}\boldsymbol{d}(\boldsymbol{Q}(t),\boldsymbol{P}(t))dt, \tag{42}$$

$$\boldsymbol{d}(\boldsymbol{q},\boldsymbol{p})=\langle\psi^{(-)}_{\boldsymbol{q}}(\boldsymbol{r})|\boldsymbol{r}|\psi^{(+)}_{\boldsymbol{p}}(\boldsymbol{r})\rangle, \tag{43}$$

where $\psi^{(-)}_{\boldsymbol{q}}(\boldsymbol{r})=[\psi^{(+)}_{-\boldsymbol{q}}(\boldsymbol{r})]^*$. The quasiclassical analysis (see Refs. [28,50]) shows that this transition happens at the times t_j, which are roots of the equation

$$\frac{\boldsymbol{P}_j^2}{2}=\frac{\boldsymbol{Q}_j^2}{2}+\Omega. \tag{44}$$

The dipole matrix element (42) with quasiclassical accuracy can be presented as

$$\mathcal{D}^{(s)}_{\rm BrS}(\boldsymbol{q},\boldsymbol{p};\Omega)=\sum_j\mathcal{D}^{(s)}_{{\rm BrS},j}(\boldsymbol{q},\boldsymbol{p};\Omega), \tag{45a}$$

$$\mathcal{D}^{(s)}_{{\rm BrS},j}(\boldsymbol{q},\boldsymbol{p};\Omega)=e^{i\Omega t_j}a^{(s)}_j(\boldsymbol{q},\boldsymbol{p})\boldsymbol{d}(\boldsymbol{Q}_j,\boldsymbol{P}_j), \tag{45b}$$

where $a^{(s)}_j(\boldsymbol{q},\boldsymbol{p})$ is given by Eq. (28c). The rescattering part of the LABrS matrix element expressed in terms of laser-field-free continuum states and the rescattering part of the laser-assisted scattering wave function (15b) is given by

$$\begin{aligned}\mathcal{D}^{(r)}_{\rm BrS}&(\boldsymbol{q},\boldsymbol{p};\Omega)\\&=\int dt e^{i[\phi_{\boldsymbol{q}}(t)-\phi_{\boldsymbol{p}}(t)+\Omega t]}\\&\times\left(\langle\psi^{(-)}_{\boldsymbol{Q}(t)}(\boldsymbol{r})|\boldsymbol{r}|\Phi^{(r)}_{\boldsymbol{p}}(\boldsymbol{r},t)\rangle+\langle\tilde{\Phi}^{(r)}_{\boldsymbol{q}}(\boldsymbol{r},t)|\boldsymbol{r}|\psi^{(+)}_{\boldsymbol{P}(t)}(\boldsymbol{r})\rangle\right).\end{aligned} \tag{46}$$

The rescattering part of the continuum state, $\tilde{\Phi}^{(r)}_{\boldsymbol{q}}(\boldsymbol{r},t)$, can be obtained from Eq. (15b) within the procedure in Eq. (39) for transformation $\Psi_{\boldsymbol{q}}(\boldsymbol{r},t)$ to $\tilde{\Psi}_{\boldsymbol{q}}(\boldsymbol{r},t)$:

$$\tilde{\Phi}^{(r)}_{\boldsymbol{q}}(\boldsymbol{r},t)=\sum_s A^{*}(\boldsymbol{Q}_s,\boldsymbol{K}'_s)a(\boldsymbol{q};t,t'_s)\psi^{(-)}_{\boldsymbol{K}_s}(\boldsymbol{r}), \tag{47}$$

where we use the reciprocity theorem for the scattering amplitude [26]. Within the saddle-point approximation and expressions (15b) and (47), the rescattering LABrS dipole moment can be approximated by

$$\begin{aligned}\mathcal{D}^{(r)}_{\rm BrS}(\boldsymbol{q},\boldsymbol{p};\Omega)&=\sum_j e^{i\Omega t_j}\mathcal{D}^{(r,1)}_{{\rm BrS},j}(\boldsymbol{q},\boldsymbol{p};\Omega),\\&\quad+\sum_j e^{i\Omega t'_j}\mathcal{D}^{(r,2)}_{{\rm BrS},j}(\boldsymbol{q},\boldsymbol{p};\Omega),\\\mathcal{D}^{(r,1)}_{{\rm BrS},j}(\boldsymbol{q},\boldsymbol{p};\Omega)&=A(\boldsymbol{K}'_j,\boldsymbol{P}'_j)\tilde{a}(\boldsymbol{p};t_j,t'_j)\boldsymbol{d}(\boldsymbol{Q}_j,\boldsymbol{K}_j),\\\mathcal{D}^{(r,2)}_{{\rm BrS},j}(\boldsymbol{q},\boldsymbol{p};\Omega)&=A(\boldsymbol{Q}_j,\boldsymbol{K}_j)\tilde{a}(\boldsymbol{q};t'_j,t_j)\boldsymbol{d}(\boldsymbol{K}'_j,\boldsymbol{P}'_j).\end{aligned} \tag{48}$$

The partial amplitude $\mathcal{D}^{(r,1)}_{{\rm BrS},j}(\boldsymbol{q},\boldsymbol{p};\Omega)$ describes the direct mechanism for LABrS [the electron is rescattered on the potential $U(r)$ and then emits the photon], while the term $\mathcal{D}^{(r,2)}_{{\rm BrS},j}(\boldsymbol{q},\boldsymbol{p};\Omega)$ describes the inverse mechanism (i.e., the electron initially emits the photon and then rescatters on the potential). In contrast to the HHG process, in which case the inverse mechanism is strongly suppressed in comparison with the direct one (see discussion in Ref. [36]), for the LABrS both terms in Eq. (48) contribute [50,51]. For the direct LABrS mechanism, the pair of times $\{t'_j,t_j\}$ is found from the system [50]

$$\boldsymbol{P}'^{\,2}_j=\boldsymbol{K}'^{\,2}_j, \tag{49a}$$

$$\frac{\boldsymbol{Q}_j^2}{2}-\frac{\boldsymbol{K}_j^2}{2}=\Omega, \tag{49b}$$

while for the inverse mechanism this pair is determined by the system

$$\frac{\boldsymbol{K}'^{\,2}_j}{2}+\Omega=\frac{\boldsymbol{P}'^{\,2}_j}{2}, \tag{50a}$$

$$\boldsymbol{Q}_j^{\,2}=\boldsymbol{K}_j^{\,2}. \tag{50b}$$

We emphasize, that the factorized analytic results for amplitudes of strong-field processes presented in this section provide the exact account of effects of the potential $U(r)$ along with quasiclassical accuracy for the account of electron-laser interaction in the adiabatic limit. The quasiclassical accuracy means that the classical action S of a free electron in the laser pulse is much larger than the Plank constant, $S\propto F^2/\omega^3\gg1$, thereby justifying the validity of the saddle-point method for the temporal integral evaluation and representation of amplitudes in terms of laser-induced classical trajectories.

B. Perturbation theory based on the adiabatic wave functions

Let $W(\boldsymbol{r},t)$ be a weak time-dependent perturbation, which we present as the sum of two terms:

$$\begin{aligned}W(\boldsymbol{r},t)&=W_+(\boldsymbol{r},t)+W_-(\boldsymbol{r},t),\\W_+(\boldsymbol{r},t)&=w(\boldsymbol{r},t)e^{-i\Omega_w t},\\W_-(\boldsymbol{r},t)&=W^{*}_+(\boldsymbol{r},t),\end{aligned} \tag{51}$$

where $w(\boldsymbol{r},t)$ is a smooth function of t [$w(\boldsymbol{r},t)\Omega_w \gg dw(\boldsymbol{r},t)/dt$]. The wave function, $\Psi_W(\boldsymbol{r},t)$, of an electron in the potential $U(r)$, an intense low-frequency field, and additional weak field [see Eq. (51)] can be presented in terms of series expansion in $W(\boldsymbol{r},t)$. In the first order in $W(\boldsymbol{r},t)$, $\Psi_W(\boldsymbol{r},t)$ is given by

$$\Psi_W(\boldsymbol{r},t) = \Psi(\boldsymbol{r},t) + \int_{-\infty}^{\infty} dt' \int d\boldsymbol{r}' \mathcal{G}(\boldsymbol{r},t;\boldsymbol{r}',t') W(\boldsymbol{r}',t') \Psi(\boldsymbol{r}',t'), \tag{52}$$

where the wave function $\Psi(\boldsymbol{r},t)$ and the Green's function $\mathcal{G}(\boldsymbol{r},t;\boldsymbol{r}',t')$ are determined by Eqs. (3) and (4). Clearly that stumbling stone in the estimation of Eq. (52) is the Green's function $\mathcal{G}(\boldsymbol{r},t;\boldsymbol{r}',t')$, whose exact explicit form can be obtained only in exceptional cases. However, the approximate expression for $\mathcal{G}(\boldsymbol{r},t;\boldsymbol{r}',t')$ can be obtained based on the functions $\Psi(\boldsymbol{r},t)$ and $\Psi_{\boldsymbol{p}}(\boldsymbol{r},t)$ [see Eqs. (8) and (15)]. Indeed, these functions are linearly independent [it can be proofed using explicit form of these functions in Eqs. (8) and (15)] and satisfy (with the quasiclassical accuracy) the TDSE (1). With these wave functions, the Green's function can be presented as follows:[3]

$$\mathcal{G}(\boldsymbol{r},t;\boldsymbol{r}',t') = -i\Big[\Psi(\boldsymbol{r},t)\Psi^*(\boldsymbol{r}',t') + (2\pi)^{-3}\int \Psi_{\boldsymbol{p}}(\boldsymbol{r},t)\Psi^*_{\boldsymbol{p}}(\boldsymbol{r}',t')d\boldsymbol{p}\Big]. \tag{53}$$

For the quasiclassical estimation of $\Psi_W(\boldsymbol{r},t)$ and transition amplitudes, we need the Green's function in two limiting cases: (i) for $t \approx t'$ and (ii) for well-separated t and t'. The first case is usable at the estimation of the temporal integral on the upper limit in Eq. (52), while the second one is utilized at the saddle-point estimation of the integral. Straightforward calculations of the Green's function using Eqs. (53), (8), and (15) show that in the first case it can be approximated by the nonstationary Green's function for the potential $U(r)$, $G_U(\boldsymbol{r},t;\boldsymbol{r}',t')$, while for well-separated times by the product of the wave functions (15) and the Volkov Green's function:

$$\mathcal{G}(\boldsymbol{r},t;\boldsymbol{r}',t') \approx \begin{cases} G_U(\boldsymbol{r},t;\boldsymbol{r}',t'), & t \approx t' \\ G_V(0,t;0,t')\psi^{(+)}_{\boldsymbol{K}}(\boldsymbol{r})[\psi^{(+)}_{\boldsymbol{K}'}(\boldsymbol{r}')]^*, & t \neq t', \end{cases}$$

$$\boldsymbol{K} \equiv \boldsymbol{K}(t,t') = \boldsymbol{A}(t) - \frac{1}{t-t'}\int_{t'}^{t} \boldsymbol{A}(\tau)\,d\tau,$$

$$\boldsymbol{K}' \equiv \boldsymbol{K}'(t,t') = \boldsymbol{A}(t') - \frac{1}{t-t'}\int_{t'}^{t} \boldsymbol{A}(\tau)\,d\tau. \tag{54}$$

Substituting the expression (54) into Eq. (52), we separate slowly ($\Psi^{(s)}_W$) and rapidly ($\Psi^{(r)}_W$) varying parts of the wave function $\Psi_W(\boldsymbol{r},t)$:

$$\Psi_W(\boldsymbol{r},t) = \Psi^{(s)}_W(\boldsymbol{r},t) + \Psi^{(r)}_W(\boldsymbol{r},t). \tag{55}$$

[3]If the potential $U(r)$ supports more than one bound state, the product of functions $\Psi(\boldsymbol{r},t)$ should be replaced by a sum over all solutions $\Psi_n(\boldsymbol{r},t)$ corresponding to bound states: $\Psi(\boldsymbol{r},t)\Psi^*(\boldsymbol{r}',t') \to \sum_n \Psi_n(\boldsymbol{r},t)\Psi^*_n(\boldsymbol{r}',t')$.

Evaluating the integral in Eq. (52) near $t' \approx t$ within the approximation (54), we obtain

$$\Psi^{(s)}_W(\boldsymbol{r},t) = e^{-iE_0 t}\Big[\varphi_0(\boldsymbol{r}) + \int G_{E_+}(\boldsymbol{r},\boldsymbol{r}')W_+(\boldsymbol{r}',t)\varphi_0(\boldsymbol{r}')\,d\boldsymbol{r}' + \int G_{E_-}(\boldsymbol{r},\boldsymbol{r}')W_-(\boldsymbol{r}',t)\varphi_0(\boldsymbol{r}')\,d\boldsymbol{r}'\Big], \tag{56}$$

where $E_\pm = E_0 \pm \Omega_w$ and $G_E(\boldsymbol{r},\boldsymbol{r}')$ is the stationary Green's function for the potential $U(r)$ with the outgoing-wave asymptotics. As is seen from Eq. (56), the slow part of the wave function is given by the superposition of the bound state and the wave packet originated due to electron interaction with the weak perturbation (51).

The time dependence of the rapidly varying part $\Psi^{(r)}_W(\boldsymbol{r},t)$ is determined by the classical action of a free electron in a laser field and can be partitioned into four terms:

$$\Psi^{(r)}_W(\boldsymbol{r},t) = e^{-iE_0 t}\Phi^{(r)}(\boldsymbol{r},t) + \sum_s a_s(t)\int G_{\mathcal{E}_+(t)}(\boldsymbol{r};\boldsymbol{r}')W_+(\boldsymbol{r}',t)\psi^{(+)}_{\boldsymbol{K}_s}(\boldsymbol{r}')\,d\boldsymbol{r}' + \sum_s a_s(t)\int G_{\mathcal{E}_-(t)}(\boldsymbol{r};\boldsymbol{r}')W_-(\boldsymbol{r}',t)\psi^{(+)}_{\boldsymbol{K}_s}(\boldsymbol{r}')\,d\boldsymbol{r}' + \sum_s g(t,\tilde{t}'_s)\psi^{(+)}_{\tilde{\boldsymbol{K}}_s}(\boldsymbol{r}), \tag{57a}$$

$$\mathcal{E}_\pm(t) = \frac{\boldsymbol{K}_s^2}{2} \pm \Omega_w, \tag{57b}$$

$$g(t,\tilde{t}'_s) = g^{(\mathrm{pr})}(t,\tilde{t}'_s)g_U(t,\tilde{t}'_s), \tag{57c}$$

$$g^{(\mathrm{pr})}(t,\tilde{t}'_s) = -\frac{1}{2\pi}\frac{e^{-iS(t,\tilde{t}'_s)}}{(t-\tilde{t}'_s)^{3/2}} \tag{57d}$$

$$g_U(t,\tilde{t}'_s) = \frac{\langle\psi^{(+)}_{\tilde{\boldsymbol{K}}'_s}(\boldsymbol{r}')|W_+(\boldsymbol{r}',\tilde{t}'_s)|\Psi_0(\boldsymbol{r}',\tilde{t}'_s)\rangle}{\sqrt{\tilde{\boldsymbol{K}}'_s\cdot\boldsymbol{F}(\tilde{t}'_s) + 2E_+(t-\tilde{t}'_s)^{-1}}},$$

$$S(t,\tilde{t}'_s) = \frac{1}{2}\int_{\tilde{t}'_s}^{t}\left[\boldsymbol{A}(\tau) - \frac{1}{t-\tilde{t}'_s}\int_{\tilde{t}'_s}^{t}\boldsymbol{A}(\xi)\,d\xi\right]^2 d\tau, \tag{57e}$$

where times $\tilde{t}'_s$ are found from the equation

$$\tilde{\boldsymbol{K}}'^{\,2}_s = 2E_+, \qquad \tilde{\boldsymbol{K}}'_s = \boldsymbol{A}(\tilde{t}'_s) - \frac{1}{t-\tilde{t}'_s}\int_{\tilde{t}'_s}^{t}\boldsymbol{A}(\xi)\,d\xi, \tag{58}$$

and $\Psi_0(\boldsymbol{r},t)$ and $\Phi^{(r)}(\boldsymbol{r},t)$ are given by Eqs. (2) and (8b). In expression (57a) for $\Psi^{(r)}_W(\boldsymbol{r},t)$, we neglect contribution from the channel, which is associated with the emission of a photon with energy Ω_w from the initial state.

In order to illustrate the application of the developed perturbation theory, we use the wave function (55) for calculation of the HHG amplitude in an intense IR field and a weak field, associated with the perturbation $W(\boldsymbol{r},t)$. For the correct calculation of the HHG amplitude, along with the wave function $\Psi_W(\boldsymbol{r},t)$ we should use the dual wave function $\tilde{\Psi}_W(\boldsymbol{r},t)$ with the ingoing-wave asymptotics at large distances

[49]. The function $\tilde{\Psi}_W(\boldsymbol{r},t)$ can be obtained from $\Psi_W(\boldsymbol{r},t)$ according to the procedure similar to described in Eq. (39). Moreover, as it was discussed in Ref. [36], in the function with the ingoing-wave assymptotics (i.e., $\tilde{\Psi}_W$) it is not necessary to use the rescattering part. As a result, for harmonics with $\Omega > E_+$ the dipole transition matrix element for the HHG is given by the expression

$$\begin{aligned}\mathbf{D}(\Omega) &= \int e^{i\Omega t}\langle\tilde{\Psi}_W^{(s)}(\boldsymbol{r},t)|\boldsymbol{r}|\Psi_W^{(r)}(\boldsymbol{r},t)\rangle\, dt \\ &= \boldsymbol{\mathcal{D}}_{\rm HHG}(\Omega) + \delta\boldsymbol{\mathcal{D}}_1^{(+)}(\Omega) + \delta\boldsymbol{\mathcal{D}}_1^{(-)}(\Omega) \\ &\quad + \delta\boldsymbol{\mathcal{D}}_2(\Omega), \end{aligned} \tag{59}$$

where $\boldsymbol{\mathcal{D}}_{\rm HHG}(\Omega)$ is determined by Eq. (19), while $\delta\boldsymbol{\mathcal{D}}_1^{(\pm)}(\Omega)$ and $\delta\boldsymbol{\mathcal{D}}_2(\Omega)$ we discuss in turn. The calculation of $\delta\boldsymbol{\mathcal{D}}_1^{(\pm)}(\Omega)$ and $\delta\boldsymbol{\mathcal{D}}_2(\Omega)$ is similar to calculations presented in Sec. IV A, so below we proceed to the final result.

The corrections $\delta\boldsymbol{\mathcal{D}}_1^{(\pm)}(\Omega)$ correspond to the emission of harmonics due to interaction between the field associated with the potential $W(\boldsymbol{r},t)$ and the electronic wave packet created by the tunneling in an intense IR field:

$$\delta\boldsymbol{\mathcal{D}}_1^{(\pm)}(\Omega) = \sum_j e^{i(\Omega+E_0)t_j}\boldsymbol{\chi}_j^{(\pm)} a_j^{(\rm tun)} a_j^{(\rm pr)}, \tag{60}$$

$$\begin{aligned}\boldsymbol{\chi}_j^{(\pm)} &= \langle\varphi_0(\boldsymbol{r})|W_\pm(\boldsymbol{r},t_j)G_{E_\mp}(\boldsymbol{r},\boldsymbol{r}')\boldsymbol{r}'|\psi_{\boldsymbol{K}_j}^{(+)}(\boldsymbol{r}')\rangle \\ &\quad + \langle\varphi_0(\boldsymbol{r})|\boldsymbol{r}G_{\mathcal{E}_\pm(t_j)}(\boldsymbol{r},\boldsymbol{r}')W_\pm(\boldsymbol{r}',t_j)|\psi_{\boldsymbol{K}_j}^{(+)}(\boldsymbol{r})\rangle\,, \end{aligned} \tag{61}$$

where the index j enumerates pairs of ionization (t_j') and recombination (t_j) events. The times t_j' and t_j are roots of the system of transcendental equations [cf. Eq. (20)]:

$$\boldsymbol{K}_j'\cdot\dot{\boldsymbol{K}}_j' = 0, \quad \boldsymbol{K}_j^2 = 2[\Omega + E_\pm], \tag{62}$$

where $\boldsymbol{K}_j'$, $\dot{\boldsymbol{K}}_j'$, and $\boldsymbol{K}_j$ are determined in Eq. (20). The explicit form of $\boldsymbol{\chi}_j^{(\pm)}$ in the Eq. (61) shows that they can be interpreted as the amplitudes of recombination (with emission of harmonic with frequency Ω) assisted by the emission or absorbtion of a photon with energy Ω_w. It should be noted that the HHG channel described by $\boldsymbol{\chi}_j^{(-)}$ contributes for harmonics with energies smaller than the maximal gained energy of an electron in IR field, so that this channel becomes significant for harmonics forbidden by the dipole selection rules in the IR field. In contrast to the correction $\delta\boldsymbol{\mathcal{D}}_1^{(-)}(\Omega)$, the term $\delta\boldsymbol{\mathcal{D}}_1^{(+)}(\Omega)$ contributes for harmonics above the cutoff of the HHG spectrum in the IR field. This channel was discussed in Refs. [52–54] and has been utilized recently for the attosecond pulse metrology [55] and time-frequency analysis of HHG by means of probe XUV pulse [56].

The last correction in the HHG amplitude (59) also can be presented in the closed analytical form

$$\delta\boldsymbol{\mathcal{D}}_2(\Omega) = \sum_j g^{(\rm pr)}(\tilde{t}_j,\tilde{t}_j')g_U(\tilde{t}_j,\tilde{t}_j')\boldsymbol{d}(\tilde{\boldsymbol{K}}_j), \tag{63}$$

where for $\boldsymbol{d}(\tilde{\boldsymbol{K}}_j)$ [see Eq. (19c)] and the pair of times $\tilde{t}_j$, $\tilde{t}_j'$ is the solution of equations

$$\tilde{\boldsymbol{K}}_j'^{\,2} = 2E_+, \quad \tilde{\boldsymbol{K}}_j' = \boldsymbol{K}'(\tilde{t}_j,\tilde{t}_j'), \tag{64a}$$

$$\tilde{\boldsymbol{K}}_j^2 = 2(\Omega + E_0), \quad \tilde{\boldsymbol{K}}_j = \boldsymbol{K}(\tilde{t}_j,\tilde{t}_j'). \tag{64b}$$

In accordance with Eq. (63), the correction $\delta\boldsymbol{\mathcal{D}}_2(\Omega)$ can be interpreted in terms of the three-step scenario of HHG. In the first step, the interaction of the bound electron with the perturbation $W(\boldsymbol{r},t)$ liberates the electron to the continuum state with momentum $\boldsymbol{K}_j'$. If $I_p > \Omega_w$, the interaction with $W(\boldsymbol{r},t)$ forms an intermediate (quasienergy) state, which decays into the continuum to the state with momentum $\boldsymbol{K}_j' \approx 0$ by the tunneling through the barrier formed by the potential $U(r)$ and IR field [57]. If $\Omega_w > I_p$, the electron appears in the continuum by absorbing the photon Ω_w with subsequent population of the continuum state with energy $E_0 + \Omega > 0$. In the second and third steps, the liberated electron propagates in the continuum and recombines to the initial state with emission of harmonic having the frequency Ω. Equation (64b) for recombination event explicitly shows that the energy of an emitted harmonic cannot exceed the maximal gained energy in the IR field, so that the correction $\delta\boldsymbol{\mathcal{D}}_2(\Omega)$ contributes for those harmonic energies, which can be effectively produced by the IR field. Finally, we should note that the magnitude of the correction $\delta\boldsymbol{\mathcal{D}}_2(\Omega)$ can be comparable with $\boldsymbol{\mathcal{D}}_{\rm HHG}(\Omega)$. Indeed, the one-photon matrix element in Eq. (57e) may have the same or larger magnitude than the tunneling exponent (11). This fact makes possible the manifestation of the term $\delta\boldsymbol{\mathcal{D}}_2(\Omega)$ in experiments (see Ref. [58]), as well as in the numerical calculations (see Refs. [58–62]).

V. SUMMARY AND OUTLOOK

In this work, we explored the analytical structure of the wave function $\Psi(\boldsymbol{r},t)$ for an electron interacting with a finite-range potential $U(r)$ and an intense low-frequency laser pulse. In our analysis of the laser-distorted wave function we considered two cases of initial conditions, when an electron is initially in a bound (i) or scattering (ii) states of the potential $U(r)$. The closed analytical forms were obtained for $\Psi(\boldsymbol{r},t)$ for both cases [see Eq. (8) for the electron in the bound state and Eq. (15) for the continuum state] and in each case $\Psi(\boldsymbol{r},t)$ was partitioned into two parts: the "slow" and "rapid." The slow part is expressed in terms of the bound state for case (i) and the scattering state with the laser-modified (kinematic) momentum for case (ii). For both cases, the rapid part of $\Psi(\boldsymbol{r},t)$ is presented as a superposition of scattering states with time-dependent asymptotic momenta [see Eqs. (8b), and (15b)], whose directions and magnitudes are determined by the classical "rescattering" condition. For case (i), the electron returns to the origin at the moment t, assuming that it appears in the continuum at the moment $t_s'(t)$. For case (ii), $t_s'(t)$ is the instant of the first electron-core collision in the presence of the laser pulse. The time-dependent coefficients in the superposition of scattering states for the rapid part of $\Psi(\boldsymbol{r},t)$ in case (i) are presented as a product of the tunneling exponent [describing the electron appearance in the continuum with minimal energy at the time $t_s'(t)$] and the time-dependent (at the time moment t) propagation factor (12) [see Eq. (8b)]. In case (ii), these coefficients involve the electron scattering amplitude (describing the electron-core collision accompanied by the energy transfer from the laser pulse to the electron) [see Eq. (15b)] instead of the tunneling factor in case (i). We emphasize that the key ingredient of the rescattering part of the laser-dressed wave function is the set of times t_s'. These

times do not depend on the shape of the potential $U(r)$ and determine the instantaneous magnitudes of the tunneling factor [for case (i)] and elastic electron scattering amplitude [for case (ii)], as well as the corresponding time-dependent propagation factors for both cases.

Based on the analytic expressions for the wave functions including the rescattering corrections, we obtain the parametrizations for transition matrix elements and cross sections for fundamental strong-field processes in terms of laser and binding-potential parameters with the exact account of effects of the potential $U(r)$ and quasiclassical accuracy for the account of electron-laser interaction (see Sec. IV A). The deduced parametrizations include aforementioned tunneling factors or scattering amplitudes and propagation factors involved in the laser-dressed state and evaluated at the particular pairs of times (t'_j, t_j) depending on the initial and final electron states.

The analytic results for the wave functions $\Psi(\boldsymbol{r}, t)$ were also utilized for the development of the perturbation theory in an additional weak field (see Sec. IV B). The perturbative result for the wave function was formulated in terms of the Green's function, whose approximate expression was obtained within the analytic expression for the adiabatic wave function $\Psi(\boldsymbol{r}, t)$. We obtained the first-order perturbative correction to $\Psi(\boldsymbol{r}, t)$ and used this result to calculate the HHG amplitude in an intense low-frequency IR field and a weak perturbation. We found that a weak perturbation leads to new channels for harmonic generation. In principle, these new HHG channels may interfere with other channels caused by an account of the perturbation in high orders. Indeed, the interaction of an atomic system with a short XUV pulse can be considered in terms of the perturbation theory even in the presence of intense IR field. In this case, the additional perturbative interaction of the XUV field with an atomic system in an intense IR field leads to the HHG channels with the absorption of the XUV photons. The harmonics produced within such channel may have an energy close to the energy of the second harmonic of the XUV field generated in the presence of IR field, so that the amplitudes with absorption of one and two XUV photons may interfere [56]. Such interference carries an information about the nonlinear interaction of an atomic system with the laser field in the XUV range, which is of the growing interest nowadays due to increasing intensities of XUV sources.

Our analytical results in this paper were obtained for a finite-range potential, so that the corresponding corrections for the Coulomb field should be taken into account applying these results for atomic systems. However, the calculation of the Coulomb corrections for the wave function is unlikely, so that these corrections can be more tractably introduced directly in transition matrix elements of fundamental processes in an intense laser field and finite-range potential. Based on the parametrizations discussed in Sec. IV A, it can be seen that the Coulomb corrections should be introduced by (i) replacing the finite-range amplitudes (the attachment, detachment, and scattering amplitudes) to the corresponding Coulomb-modified counterparts and (ii) introducing quasiclassical Coulomb corrections at the subbarrier electron motion and propagation in the continuum. Although the general conception of Coulomb corrections was formulated in Refs. [63–66], the practical realization with subsequent testing of their accuracy is still a challenge for a strong-field process in a tailored laser pulse.

ACKNOWLEDGMENTS

This work was supported in part by the Russian Science Foundation through Grant No. 20-11-20289 (analytical calculations for initially bound electron, the calculation of HHG amplitude, and developing of perturbation theory in an intense laser field) and by the Ministry of Education and Science of the Russian Federation through Project No. FZGU-2020-0035 (A.V.F. and N.L.M.). The authors thank Tatyana Sarantseva for fruitful discussions and Alexander Romanov and Nikolai Vvedenskii for providing us with the numerical TDSE results for the HHG yield in Fig. 3.

APPENDIX A: DERIVATION OF EQ. (5)

In this Appendix we use Dirac's notations for shortness of intermediate expressions. The nonstationary retarded Green's function for the Hamiltonian $\hat{H}(\boldsymbol{r}, t)$, $\mathcal{G} \equiv \mathcal{G}(\boldsymbol{r}, t; \boldsymbol{r}', t')$, satisfies the Dyson relation for Green's functions:

$$\mathcal{G} = G_V + G_V U \mathcal{G}, \tag{A1}$$

where the retarded Volkov Green's function, $G_V \equiv G_V(\boldsymbol{r}, t; \boldsymbol{r}', t')$, is given by Eq. (6) and the short notation $G_V U \mathcal{G}$ means

$$G_V U \mathcal{G} \equiv \int_{-\infty}^{\infty} dt'' \int d\boldsymbol{r}'' G_V(\boldsymbol{r}, t; \boldsymbol{r}'', t'') \times U(\boldsymbol{r}'') \mathcal{G}(\boldsymbol{r}'', t''; \boldsymbol{r}', t').$$

Substituting Eq. (A1) into Eq. (3), we obtain

$$\begin{aligned} |\Psi\rangle &= |\Psi_0\rangle + |\mathcal{G} V \Psi_0\rangle \\ &= |\Psi_0\rangle + |G_V V \Psi_0\rangle + |G_V U \underbrace{\mathcal{G} V \Psi_0\rangle}_{|\Psi\rangle - |\Psi_0\rangle} \\ &= |\Psi_0\rangle + |G_V V \Psi_0\rangle + |G_V U \Psi\rangle - |G_V U \Psi_0\rangle. \end{aligned} \tag{A2}$$

For further transformation of Eq. (A2), we use the well-known relation for a stationary wave function [68]:

$$|\Psi_0\rangle = \{|\varphi_0\rangle\} + |G_0 U \Psi_0\rangle, \tag{A3}$$

where $\{|\varphi_0\rangle\}$ is zero if $|\Psi_0\rangle$ belongs to the discrete spectrum and $\{|\varphi_0\rangle\} \equiv |\varphi_0\rangle$ is an eigenvector of the kinetic energy operator (i.e., a plane-wave state) if $|\Psi_0\rangle$ belongs to the continuum spectrum, and G_0 is the nonstationary Green's function for a free electron. Substituting (A3) into the second term of Eq. (A2), we obtain

$$\begin{aligned} |\Psi\rangle &= |\Psi_0\rangle + \{|G_V V \varphi_0\rangle\} + |\underbrace{G_V V G_0}_{G_V - G_0} U \Psi_0\rangle \\ &\quad + |G_V U \Psi\rangle - |G_V U \Psi_0\rangle \\ &= \underbrace{\{|\varphi_0\rangle + |G_V V \varphi_0\rangle\}}_{|\psi_V\rangle} + |G_V U \Psi\rangle \\ &= \{|\psi_V\rangle\} + |G_V U \Psi\rangle, \end{aligned} \tag{A4}$$

where $|\psi_V\rangle$ is the Volkov state of a free electron in a laser field. The first term (the term in braces) in Eq. (A4) should

be omitted if $|\Psi_0\rangle$ represents a bound state. Equation (A4) is equivalent to Eq. (5).

APPENDIX B: DERIVATION OF EQS. (8) AND (15)

1. The case of initial bound state $\varphi_0(\mathbf{r})$

We seek the solution of Eq. (5) in the form

$$\Psi(\boldsymbol{r},t) = e^{-iE_0 t}\,\Phi(\boldsymbol{r},t).$$

Within Eqs. (5) and (6), the function $\Phi(\boldsymbol{r},t)$ can be presented in terms of a function $f(\boldsymbol{p},t')$ [34]:

$$\Phi(\boldsymbol{r},t) = -i\int d\boldsymbol{p}\int_{-\infty}^{t} dt'\, e^{i[\boldsymbol{P}(t)\cdot\boldsymbol{r}+S(\boldsymbol{p};t,t')]} f(\boldsymbol{p},t'), \quad \text{(B1)}$$

$$f(\boldsymbol{p},t) = \frac{1}{(2\pi)^3}\int e^{-i\boldsymbol{P}(t)\cdot\boldsymbol{r}} U(\boldsymbol{r})\Phi(\boldsymbol{r},t)\,d\boldsymbol{r},$$

$$S(\boldsymbol{p};t,t') = E_0(t-t') - \frac{1}{2}\int_{t'}^{t} \boldsymbol{P}^2(\tau)\,d\tau. \quad \text{(B2)}$$

The function $f(\boldsymbol{p},t)$ is the key object in the evaluation of the function $\Phi(\boldsymbol{r},t)$ in the low-frequency (or adiabatic) limit, which is ensured by inequalities $F^2/\omega^3 \gg 1$ and $I_p/\omega \gg 1$, where F and ω give the order of magnitude for the electric field strength and carrier frequency of a strong low-frequency laser pulse, and I_p is the detachment threshold ($E_0 = -I_p$). We note that in the low-frequency limit, the laser-induced population of exited states is negligibly small[4] [67] and the initial state can be considered as isolated (we do not consider the laser-induced resonances between atomic levels, which require a special consideration for the low-frequency fields). In the adiabatic limit, the function $f(\boldsymbol{p},t)$ can be presented as a sum of the slowly varying in time function $f^{(s)}(\boldsymbol{p},t)$ and rapidly oscillating function $f^{(r)}(\boldsymbol{p},t)$:

$$f(\boldsymbol{p},t) = f^{(s)}(\boldsymbol{p},t) + f^{(r)}(\boldsymbol{p},t). \quad \text{(B3)}$$

The function $f^{(s)}(\boldsymbol{p},t)$ is expressed in terms of the function $f_0(\boldsymbol{p})$, which determines the initial bound state $\varphi_0(\boldsymbol{r})$ [34]:

$$\varphi_0(\boldsymbol{r}) = \int e^{i\boldsymbol{p}\cdot\boldsymbol{r}}\frac{f_0(\boldsymbol{p})}{E_0 - p^2/2}\,d\boldsymbol{p}, \quad \text{(B4a)}$$

$$f^{(s)}(\boldsymbol{p},t) = f_0(\boldsymbol{P}(t)). \quad \text{(B4b)}$$

The function $f^{(r)}(\boldsymbol{p},t)$ has the form [34]

$$f^{(r)}(\boldsymbol{p},t) = \sqrt{\frac{2\pi}{i}}\sum_s \int \frac{e^{iS(\boldsymbol{k};t,t'_s)}}{\sqrt{\alpha_s}} \times T(\boldsymbol{P}(t),\boldsymbol{K}(t)) f_0(\boldsymbol{K}(t'_s))\,d\boldsymbol{k},$$

$$\alpha_s = \frac{\partial^2 S(\boldsymbol{k};t,t'_s)}{\partial t'^2_s} = -\boldsymbol{K}(t'_s)\cdot\boldsymbol{F}(t'_s), \quad \text{(B5)}$$

where times $t'_s \equiv t'_s(\boldsymbol{k},t)$ are found from the equation

$$\boldsymbol{K}^2(t'_s) = 2E_0, \quad \boldsymbol{K}(t) = \boldsymbol{k} + \boldsymbol{A}(t). \quad \text{(B6)}$$

In Eq. (B5) the effects of electron-core interaction are presented by two factors: the function $f_0(\boldsymbol{K}(t'_s))$ and the half-shell T-matrix $T(\boldsymbol{P}(t),\boldsymbol{K}(t))$. The T-matrix $T(\boldsymbol{p},\boldsymbol{k})$ describes the electron scattering on the potential $U(r)$ with momentum exchange from $\boldsymbol{k}$ to $\boldsymbol{p}$ [68]:

$$T(\boldsymbol{p},\boldsymbol{k}) = \frac{1}{(2\pi)^3}\int e^{-i\boldsymbol{p}\cdot\boldsymbol{r}} U(r)\psi^{(+)}_{\boldsymbol{k}}(\boldsymbol{r})\,d\boldsymbol{r}, \quad \text{(B7)}$$

where $\psi^{(+)}_{\boldsymbol{k}}(\boldsymbol{r})$ is the scattering state of an electron with the momentum $\boldsymbol{k}$ in the potential $U(r)$ having the asymptotics of outgoing waves.

The calculation of transition matrix elements for strong-field phenomena is performed mostly in the coordinate space, in which case the explicit form of $\Phi(\boldsymbol{r},t)$ is necessary. We show that expression for $\Phi(\boldsymbol{r},t)$ can be deduced in the closed analytic form and expressed in terms of functions $\varphi_0(\boldsymbol{r})$ and $\psi^{(+)}_{\boldsymbol{k}}(\boldsymbol{r})$. Let us substitute the expression (B3) into Eq. (B1) and express the wave function $\Phi(\boldsymbol{r},t)$ in terms of functions $\varphi^{(s)}(\boldsymbol{k},t)$ and $\varphi^{(r)}(\boldsymbol{k},t)$:

$$\Phi(\boldsymbol{r},t) = \int e^{i\boldsymbol{K}(t)\cdot\boldsymbol{r}}\varphi^{(s)}(\boldsymbol{k},t)\,d\boldsymbol{k} + \int e^{i\boldsymbol{P}(t)\cdot\boldsymbol{r}}\varphi^{(r)}(\boldsymbol{p},t)\,d\boldsymbol{p}, \quad \text{(B8)}$$

where

$$\varphi^{(s)}(\boldsymbol{k},t) = -i\int_{-\infty}^{t} e^{iS(\boldsymbol{k};t,t')} f^{(s)}(\boldsymbol{k},t')\,dt', \quad \text{(B9a)}$$

$$\varphi^{(r)}(\boldsymbol{p},t) = -i\int_{-\infty}^{t} e^{iS(\boldsymbol{p};t,t')} f^{(r)}(\boldsymbol{p},t')\,dt'. \quad \text{(B9b)}$$

In the low-frequency approximation, the temporal integrals in Eqs. (B9) can be analytically estimated. There are two contributions in integrals (B9) (see, e.g., Ref. [69]): (i) the contribution from the vicinity of the upper limit and (ii) the contribution from saddle points t'_s [see Eq. (B6)].

For the integral (B9a), the estimation near the upper limit is achieved by approximating the integrand in Eq. (B9a) near $t' = t$ within substitutions:

$$S(\boldsymbol{k};t,t') \approx \left[E_0 - \frac{\boldsymbol{K}^2(t)}{2}\right](t-t'),$$

$$f^{(s)}(\boldsymbol{k},t') = f_0(\boldsymbol{K}(t')) \approx f_0(\boldsymbol{K}(t)),$$

and evaluating the integral in t' [we mark this contribution to the integral (B9a) as $\varphi^{(s)}_0(\boldsymbol{p},t)$]:

$$\varphi^{(s)}_0(\boldsymbol{k},t) = \frac{f_0(\boldsymbol{K}(t))}{E_0 - \boldsymbol{K}^2(t)/2}. \quad \text{(B10)}$$

Integration over $\boldsymbol{k}$ of the function $\varphi^{(s)}_0(\boldsymbol{k},t)$ with the weight function $e^{i\boldsymbol{K}(t)\cdot\boldsymbol{r}}$ in Eq. (B8) can be performed by taking into account the equality (B4a)

$$\int e^{i\boldsymbol{K}(t)\cdot\boldsymbol{r}}\varphi^{(s)}_0(\boldsymbol{K}(t),t)\,d\boldsymbol{k} = \varphi_0(\boldsymbol{r}). \quad \text{(B11)}$$

Estimating integral (B9a) for $\varphi^{(s)}(\boldsymbol{k},t)$ by the saddle-point method [we mark this contribution to the integral (B9a) as $\varphi^{(s)}_1(\boldsymbol{k},t)$], we obtain

$$\varphi^{(s)}_1(\boldsymbol{k},t) = \sqrt{\frac{2\pi}{i}}\sum_s \frac{e^{iS(\boldsymbol{k};t,t'_s)}}{\sqrt{\alpha_s}} f_0(\boldsymbol{K}(t'_s)), \quad \text{(B12)}$$

[4]The exponentially small population of exited states in a short-range potential cannot affect strong-field phenomena considered here [see discussion of Fig. 3(b) in Sec. IV A 1].

where the summation is taken for all appropriate solutions of Eq. (B6).

Let us further estimate the function $\varphi^{(r)}(\boldsymbol{p},t)$ in Eq. (B9b):

$$\varphi^{(r)}(\boldsymbol{p},t) = -i\sqrt{\frac{2\pi}{i}}\sum_s \int d\boldsymbol{k}\,\frac{e^{iS(\boldsymbol{k};t,t'_s)}f_0(\boldsymbol{K}(t'_s))}{\sqrt{\alpha_s}} \times \int_{-\infty}^{t} dt'\, e^{\frac{i}{2}\int_{t'}^{t}[\boldsymbol{K}^2(\tau)-\boldsymbol{P}^2(\tau)]\,d\tau} T(\boldsymbol{P}(t'),\boldsymbol{K}(t')). \tag{B13}$$

We evaluate the integral in second line of Eq. (B13) near the vicinity of the upper limit $t'=t$ [we mark this contribution as $\varphi_1^{(r)}(\boldsymbol{p},t)$], while we neglect the contribution from saddle points, which gives the second-order correction of the exponential smallness caused by the imaginary part of t'_s. As a result, we obtain

$$\varphi_1^{(r)}(\boldsymbol{p},t) = \sqrt{\frac{2\pi}{i}}\sum_s \int \frac{e^{iS(\boldsymbol{k};t,t'_s)}f_0(\boldsymbol{K}(t'_s))}{\sqrt{\alpha_s}} \times \frac{2T(\boldsymbol{P}(t),\boldsymbol{K}(t))}{\boldsymbol{K}^2(t)-\boldsymbol{P}^2(t)+i0}\,d\boldsymbol{k}, \tag{B14}$$

where the sign of an infinitesimal ensures both the convergence of the temporal integral in Eq. (B13) and outgoing-wave behavior at large distances for $\Phi(\boldsymbol{r},t)$.

In the next, we combine together the integrated results for $\varphi_1^{(s)}(\boldsymbol{k},t)$ and $\varphi_1^{(r)}(\boldsymbol{p},t)$:

$$\begin{aligned}\Phi^{(r)}(\boldsymbol{r},t) &= \int e^{i\boldsymbol{K}(t)\cdot\boldsymbol{r}}\varphi_1^{(s)}(\boldsymbol{k},t)\,d\boldsymbol{k} + \int e^{i\boldsymbol{P}(t)\cdot\boldsymbol{r}}\varphi_1^{(r)}(\boldsymbol{p},t)\,d\boldsymbol{p}\\ &= \sqrt{\frac{2\pi}{i}}\sum_s \int d\boldsymbol{k}\frac{e^{iS_{E_0}(\boldsymbol{k};t,t'_s)}}{\sqrt{\alpha_s}} f_{E_0}^{(0)}(\boldsymbol{K}(t'_s))\\ &\quad\times\left[e^{i\boldsymbol{K}(t)\cdot\boldsymbol{r}} + 2\int e^{i\boldsymbol{P}(t)\cdot\boldsymbol{r}}\frac{T(\boldsymbol{P}(t),\boldsymbol{K}(t))}{\boldsymbol{K}(t)^2-\boldsymbol{P}(t)^2+i0}\,d\boldsymbol{p}\right].\end{aligned}$$

Taking into account the well-known expression in the scattering theory [68]

$$\psi_{\boldsymbol{k}}^{(+)}(\boldsymbol{r}) = e^{i\boldsymbol{k}\cdot\boldsymbol{r}} + 2\int e^{i\boldsymbol{p}\cdot\boldsymbol{r}}\frac{T(\boldsymbol{p},\boldsymbol{k})}{k^2-p^2+i0}\,d\boldsymbol{p}, \tag{B15}$$

we obtain $\Phi(\boldsymbol{r},t)$ and $\Phi^{(r)}(\boldsymbol{r},t)$ in the form

$$\Phi(\boldsymbol{r},t) = \varphi_0(\boldsymbol{r}) + \Phi^{(r)}(\boldsymbol{r},t), \tag{B16a}$$

$$\Phi^{(r)}(\boldsymbol{r},t) = \sqrt{\frac{2\pi}{i}}\sum_s \int \frac{e^{iS(\boldsymbol{k};t,t'_s)}}{\sqrt{\alpha_s}} \times f_0(\boldsymbol{K}(t'_s))\psi_{\boldsymbol{K}(t)}^{(+)}(\boldsymbol{r})\,d\boldsymbol{k}. \tag{B16b}$$

The further simplification is achieved by applying adiabatic approximation to Eq. (B16b), which consists in the evaluating integral in $\boldsymbol{k}$ by saddle-point method and series expansion of $S(\boldsymbol{k};t,t'_s)$ in imaginary part of t'_s (see Ref. [34] for details). After these calculations the wave function $\Phi(\boldsymbol{r},t)$ can be approximated by expression (8).

2. The case of initial continuum state

The case of initial electron in the continuum state with asymptotic momentum $\boldsymbol{p}$ is considered similarly to the case of bound electron, which we have discussed above. In this case the wave function can be presented in the form

$$\Psi(\boldsymbol{r},t) = e^{-\frac{i}{2}\int^t \boldsymbol{P}^2(\tau)\,d\tau}\Phi_{\boldsymbol{p}}(\boldsymbol{r},t), \tag{B17}$$

where

$$\Phi_{\boldsymbol{p}}(\boldsymbol{r},t) = e^{i\boldsymbol{P}(t)\cdot\boldsymbol{r}} - i\int d\boldsymbol{k}\int_{-\infty}^{t} dt' e^{i[\boldsymbol{K}(t)\cdot\boldsymbol{r}+S(\boldsymbol{p},\boldsymbol{k};t,t')]}f_{\boldsymbol{p}}(\boldsymbol{k};t'), \tag{B18a}$$

$$S(\boldsymbol{p},\boldsymbol{k};t,t') = \frac{1}{2}\int_{t'}^{t}\left[\boldsymbol{P}^2(\tau)-\boldsymbol{K}^2(\tau)\right]d\tau, \tag{B18b}$$

$$f_{\boldsymbol{p}}(\boldsymbol{k},t) = \frac{1}{(2\pi)^3}\int e^{-i\boldsymbol{K}(t)\cdot\boldsymbol{r}}U(\boldsymbol{r})\Phi_{\boldsymbol{p}}(\boldsymbol{r},t)\,d\boldsymbol{r}. \tag{B18c}$$

The function $f_{\boldsymbol{p}}(\boldsymbol{k},t)$ satisfies the equation

$$\begin{aligned}f_{\boldsymbol{p}}(\boldsymbol{k};t) &= u(\boldsymbol{k}-\boldsymbol{p}) - i\int d\boldsymbol{q}\,u(\boldsymbol{k}-\boldsymbol{q})\\ &\quad\times\int_{-\infty}^{t} dt' e^{iS(\boldsymbol{p},\boldsymbol{q};t,t')}f_{\boldsymbol{p}}(\boldsymbol{q};t'),\\ u(\boldsymbol{k}-\boldsymbol{p}) &= \frac{1}{(2\pi)^3}\int e^{-i(\boldsymbol{k}-\boldsymbol{p})\cdot\boldsymbol{r}}U(r)\,d\boldsymbol{r}.\end{aligned} \tag{B19}$$

The analysis of Eq. (B19) is similar to presented in Ref. [34]. The function $f_{\boldsymbol{p}}(\boldsymbol{k};t)$ is partitioned into "slow," $f_{\boldsymbol{p}}^{(s)}(\boldsymbol{k},t)$, and "rapid," $f_{\boldsymbol{p}}^{(r)}(\boldsymbol{k},t)$, terms:

$$f_{\boldsymbol{p}}(\boldsymbol{k};t) = f_{\boldsymbol{p}}^{(s)}(\boldsymbol{k};t) + f_{\boldsymbol{p}}^{(r)}(\boldsymbol{k};t). \tag{B20}$$

The slow part follows from Eq. (B19) by estimating temporal integral near the upper limit:

$$\begin{aligned}f_{\boldsymbol{p}}^{(s)}(\boldsymbol{k};t) &= u(\boldsymbol{k}-\boldsymbol{p}) + 2\int\frac{u(\boldsymbol{k}-\boldsymbol{q})f_{\boldsymbol{p}}^{(s)}(\boldsymbol{q};t)}{\boldsymbol{P}^2(t)-\boldsymbol{Q}^2(t)}\,d\boldsymbol{q},\\ \boldsymbol{Q}(t) &= \boldsymbol{q}+\boldsymbol{A}(t).\end{aligned} \tag{B21}$$

Since $\boldsymbol{k}-\boldsymbol{p} = \boldsymbol{K}(t)-\boldsymbol{P}(t)$ and $\boldsymbol{k}-\boldsymbol{q} = \boldsymbol{K}(t)-\boldsymbol{Q}(t)$, Eq. (B21) coincides with the integral equation for the half-shell T-matrix [68], so that $f_{\boldsymbol{p}}^{(s)}(\boldsymbol{k},t)$ is expressed in terms of the T-matrix with instantaneous laser-modified momenta:

$$f_{\boldsymbol{p}}^{(s)}(\boldsymbol{k};t) = T(\boldsymbol{K}(t),\boldsymbol{P}(t)). \tag{B22}$$

The equation for the rapid part, $f_{\boldsymbol{p}}^{(r)}(\boldsymbol{k},t)$, is deduced from Eq. (B19) in the same manner as in Ref. [34], so we proceed to the final result for $f_{\boldsymbol{p}}^{(r)}(\boldsymbol{k},t)$, which can be obtained from Eq. (B5) by formal replacements:

$$\begin{aligned}&\boldsymbol{k}\to\boldsymbol{q},\\ &S(\boldsymbol{k};t,t'_s)\to S(\boldsymbol{p},\boldsymbol{q};t,t'_s),\\ &f_0(\boldsymbol{K}(t'_s))\to f_{\boldsymbol{p}}^{(s)}(\boldsymbol{q},t'_s),\\ &\alpha_s\to\boldsymbol{F}(t'_s)\cdot(\boldsymbol{p}-\boldsymbol{q}),\end{aligned}$$

where t_s' is found from the transcendental saddle-point equation:

$$\boldsymbol{P}^2(t_s') = \boldsymbol{Q}^2(t_s'). \tag{B23}$$

As a result, we obtain $f_{\boldsymbol{p}}^{(r)}(\boldsymbol{k}, t)$:

$$f_{\boldsymbol{p}}^{(r)}(\boldsymbol{k}, t) = \sqrt{\frac{2\pi}{i}} \sum_s \int \frac{e^{iS(\boldsymbol{p},\boldsymbol{q};t,t_s')}}{\sqrt{\boldsymbol{F}(t_s') \cdot (\boldsymbol{p} - \boldsymbol{q})}} \times T(\boldsymbol{K}(t), \boldsymbol{Q}(t))\, T(\boldsymbol{Q}(t_s'), \boldsymbol{P}(t_s'))\, d\boldsymbol{q}. \tag{B24}$$

We note, that in accordance with the saddle-point equation (B23), the T-matrix $T(\boldsymbol{Q}(t_s'), \boldsymbol{P}(t_s'))$ in Eq. (B24) is taken on the energy shell, so that it can be expressed in terms of the elastic scattering amplitude $A(\boldsymbol{Q}(t_s'), \boldsymbol{P}(t_s'))$:

$$T(\boldsymbol{Q}(t_s'), \boldsymbol{P}(t_s')) = -\frac{1}{4\pi^2} A(\boldsymbol{Q}(t_s'), \boldsymbol{P}(t_s')). \tag{B25}$$

The equality Eq. (B25) is valid for the classically allowed region of electron momenta $\boldsymbol{p}$[5], which ensures the real-valued scattering times t_s'. For the classically forbidden region of $\boldsymbol{p}$ the analytic continuation for the scattering amplitude should be applied.

Substituting the expession (B20) into Eq. (B18a) and using the low-frequency results (B22) and (B24), we obtain the adiabatic result for $\Phi_{\boldsymbol{p}}(\boldsymbol{r}, t)$:

$$\Phi_{\boldsymbol{p}}(\boldsymbol{r}, t) = \Phi_{\boldsymbol{p}}^{(0)}(\boldsymbol{r}, t) + \Phi_{\boldsymbol{p}}^{(r)}(\boldsymbol{r}, t). \tag{B26}$$

In Eq. (B26) the term $\Phi_{\boldsymbol{p}}^{(0)}(\boldsymbol{r}, t)$ represents the adiabatic result in the lowest order and coincides with the well-known Kroll-Watson low-frequency result for the scattering state [27]:

$$\Phi_{\boldsymbol{p}}^{(0)}(\boldsymbol{r}, t) = \psi_{\boldsymbol{P}(t)}^{(+)}(\boldsymbol{r}), \tag{B27}$$

where $\psi_{\boldsymbol{P}(t)}^{(+)}(\boldsymbol{r})$ is the scattering state in the potential $U(r)$ with instantaneous momentum $\boldsymbol{P}(t)$. To obtain the result (B27), we estimated the temporal integral in Eq. (B18a) taking into account only the vicinity of the point $t' = t$ and approximating $f_{\boldsymbol{p}}^{(s)}(\boldsymbol{k}, t') \approx f_{\boldsymbol{p}}^{(s)}(\boldsymbol{k}, t)$. The second term, $\Phi_{\boldsymbol{p}}^{(r)}(\boldsymbol{r}, t)$, in Eq. (B26) is the rescattering correction to the Kroll-Watson wave function:

$$\Phi_{\boldsymbol{p}}^{(r)}(\boldsymbol{r}, t) = \left(\frac{i}{2\pi}\right)^{3/2} \int \sum_s \frac{e^{iS(\boldsymbol{p},\boldsymbol{k};t,t_s')}}{\sqrt{\boldsymbol{F}(t_s') \cdot (\boldsymbol{p} - \boldsymbol{k})}} \times A(\boldsymbol{K}(t_s'), \boldsymbol{P}(t_s'))\, \psi_{\boldsymbol{K}(t)}^{(+)}(\boldsymbol{r})\, d\boldsymbol{k}. \tag{B28}$$

The result (B28) is obtained taking into account the saddle-point contribution to the temporal integral in Eq. (B18a) for the term containing $f^{(s)}$ and the contribution of point $t' = t$ for the term containing $f^{(r)}$ [cf. the derivation of the rescattering result (B16b) for the initial bound state in the potential $U(r)$]. Finally, evaluating the integral over k in Eq. (B28) by the saddle-point method, we obtain Eq. (15).

[5] In the considered case, the classically allowed region of electron momenta means, that the transmitted energy $\boldsymbol{A}(t_s') \cdot (\boldsymbol{q} - \boldsymbol{p})$ in the laser field does not exceed the difference between the final $(k^2/2)$ and initial $(p^2/2)$ electron energies: $2\boldsymbol{A}(t_s') \cdot (\boldsymbol{q} - \boldsymbol{p}) \leqslant k^2 - p^2$.

[1] D. B. Milošević and F. Ehlotzky, Scattering and reaction processes in powerful laser fields, Adv. At. Mol. Opt. Phys. **49**, 373 (2003).

[2] A. Becker and F. H. M. Faisal, Intense-field many-body S-matrix theory, J. Phys. B: At. Mol. Opt. Phys. **38**, R1 (2005).

[3] D. Bauer and P. Koval, Qprop: A Schrödinger-solver for intense laser-atom interaction, Comput. Phys. Commun. **174**, 396 (2006).

[4] S. Patchkovskii and H. G. Muller, Simple, accurate, and efficient implementation of 1-electron atomic time-dependent Schrödinger equation in spherical coordinates, Comput. Phys. Commun. **199**, 153 (2016).

[5] W. Becker, F. Grasbon, R. Kopold, D. B. Milošević, G. G. Paulus, and H. Walther, Above threshold ionization: From classical features to quantum effects, Adv. At. Mol. Opt. Phys. **48**, 35 (2002).

[6] M. V. Frolov, A. A. Khuskivadze, N. L. Manakov, and A. F. Starace, An analytical quantum model for intense field processes: Quantum origin of rescattering plateaus, J. Phys. B: At. Mol. Opt. Phys. **39**, S283 (2006).

[7] A. Galstyan, O. Chuluunbaatar, A. Hamido, Yu. V. Popov, F. Mota-Furtado, P. F. O'Mahony, N. Janssens, F. Catoire, and B. Piraux, Reformulation of the strong-field approximation for light-matter interactions, Phys. Rev. A **93**, 023422 (2016).

[8] Y. Popov, A. Galstyan, F. Mota-Furtado, P. F. O'Mahony, and B. Piraux, Strong field approximation within a Faddeev-like formalism for laser-matter interactions, Eur. Phys. J. D **71**, 93 (2017).

[9] P. Salières, B. Carré, L. Le Déroff, F. Grasbon, G. G. Paulus, H. Walther, R. Kopold, W. Becker, D. B. Milošević, A. Sanpera, and M. Lewenstein, Feynman's path-integral approach for intense-laser-atom interactions, Science **292**, 902 (2001).

[10] P. B. Corkum, Plasma Perspective on Strong Field Multiphoton Ionization, Phys. Rev. Lett. **71**, 1994 (1993).

[11] W. Becker, A. Lohr, and M. Kleber, Effects of rescattering on above-threshold ionization, J. Phys. B: At. Mol. Opt. Phys. **27**, L325 (1994).

[12] J. Itatani, J. Levesque, D. Zeidler, H. Niikura, H. Pépin, J. C. Kieffer, P. B. Corkum, and D. M. Villeneuve, Tomographic imaging of molecular orbitals, Nature (London) **432**, 867 (2004).

[13] J. Levesque, D. Zeidler, J. P. Marangos, P. B. Corkum, and D. M. Villeneuve, High Harmonic Generation and the Role of Atomic Orbital Wave Functions, Phys. Rev. Lett. **98**, 183903 (2007).

[14] X. X. Zhou, Z. Chen, T. Morishita, A.-T. Le, and C. D. Lin, Retrieval of electron-atom scattering cross sections from laser-induced electron rescattering of atomic negative ions in intense laser fields, Phys. Rev. A **77**, 053410 (2008).

[15] C. D. Lin, A.-T. Le, Z. Chen, T. Morishita, and R. Lucchese, Strong-field rescattering physics—Self-imaging of a molecule by its own electrons, J. Phys. B: At. Mol. Opt. Phys. **43**, 122001 (2010).

[16] M. V. Frolov, N. L. Manakov, T. S. Sarantseva, M. Yu. Emelin, M. Yu. Ryabikin, and A. F. Starace, Analytic Description of the High-Energy Plateau in Harmonic Generation by Atoms: Can the Harmonic Power Increase with Increasing Laser Wavelengths? Phys. Rev. Lett. **102**, 243901 (2009).

[17] M. V. Frolov, N. L. Manakov, and A. F. Starace, Potential barrier effects in high-order harmonic generation by transition-metal ions, Phys. Rev. A **82**, 023424 (2010).

[18] A. D. Shiner, B. E. Schmidt, C. Trallero-Herrero, H. J. Wörner, S. Patchkovskii, P. B. Corkum, J.–C. Kieffer, F. Légaré, and D. M. Villeneuve, Probing collective multi-electron dynamics in xenon with high-harmonic spectroscopy, Nat. Phys. **7**, 464 (2011).

[19] A. D. Shiner, B. E. Schmidt, C. Trallero-Herrero, P. B. Corkum, J.-C. Kieffer, F. Légaré, and D. M. Villeneuve, Observation of Cooper minimum in krypton using high harmonic spectroscopy, J. Phys. B: At. Mol. Opt. Phys. **45**, 074010 (2012).

[20] A. A. Romanov, A. A. Silaev, M. V. Frolov, and N. V. Vvedenskii, Influence of the polarization of a multielectron atom in a strong laser field on high-order harmonic generation, Phys. Rev. A **101**, 013435 (2020).

[21] A. A. Romanov, A. A. Silaev, T. S. Sarantseva, M. V. Frolov, and N. V. Vvedenskii, Study of high-order harmonic generation in xenon based on time-dependent density-functional theory, New J. Phys. **23**, 043014 (2021).

[22] X.-Y. Lai, C. Poli, H. Schomerus, and C. Figueira de Morisson Faria, Influence of the Coulomb potential on above-threshold ionization: A quantum-orbit analysis beyond the strong-field approximation, Phys. Rev. A **92**, 043407 (2015).

[23] D. B. Milošević, Semiclassical approximation for strong-laser-field processes, Phys. Rev. A **96**, 023413 (2017).

[24] R. P. Feynman and A. R. Hibbs, *Quantum Mechanics and Path Integrals* (McGraw-Hill, New York, 1965).

[25] M. C. Gutzwiller, Phase-integral approximation in momentum space and the bound states of an atom, J. Math. Phys. **8**, 1979 (1967).

[26] L. D. Landau and E. M. Lifshitz, *Quantum Mechanics (Non-relativistic Theory)* (Pergamon Press, Oxford, 1977).

[27] N. M. Kroll and K. M. Watson, Charged-particle scattering in the presence of a strong electromagnetic wave, Phys. Rev. A **8**, 804 (1973).

[28] F. Zhou and L. Rosenberg, Bremsstrahlung in laser-assisted scattering, Phys. Rev. A **48**, 505 (1993).

[29] M. Pont, R. M. Potvliege, R. Shakeshaft, and Z.-J. Teng, Low-frequency theory of multiphoton ionization. II. General formulation and further results for ionization of H(1*s*), Phys. Rev. A **45**, 8235 (1992).

[30] A. I. Baz', Ya. B. Zel'dovich, and A. M. Perelomov, *Scattering, Reactions and Decays in Nonrelativistic Quantum Mechanics*, 2nd ed. (Nauka, Moscow, 1971).

[31] O. I. Tolstikhin and T. Morishita, Adiabatic theory of ionization by intense laser pulses: Finite-range potentials, Phys. Rev. A **86**, 043417 (2012).

[32] Y. Okajima, O. I. Tolstikhin, and T. Morishita, Adiabatic theory of high-order harmonic generation: One-dimensional zero-range-potential model, Phys. Rev. A **85**, 063406 (2012).

[33] A. de Bohan, B. Piraux, L. Ponce, R. Taïeb, V. Véniard, and A. Maquet, Direct and Indirect Pathways in Strong Field Atomic Ionization Dynamics, Phys. Rev. Lett. **89**, 113002 (2002).

[34] A. V. Flegel, N. L. Manakov, A. V. Sviridov, M. V. Frolov, L. Geng, and L.-Y. Peng, Analytic description of the above-threshold detachment in the adiabatic limit, Phys. Rev. A **102**, 063119 (2020).

[35] G. F. Gribakin and M. Yu. Kuchiev, Multiphoton detachment of electrons from negative ions, Phys. Rev. A **55**, 3760 (1997).

[36] M. Yu. Kuchiev and V. N. Ostrovsky, Quantum theory of high harmonic generation as a three-step process, Phys. Rev. A **60**, 3111 (1999).

[37] M. V. Frolov, N. L. Manakov, E. A. Pronin, and A. F. Starace, Model-Independent Quantum Approach for Intense Laser Detachment of a Weakly Bound Electron, Phys. Rev. Lett. **91**, 053003 (2003).

[38] S. Beiser, M. Klaiber, and I. Yu. Kiyan, Photodetachment in a strong circularly polarized laser field, Phys. Rev. A **70**, 011402(R) (2004).

[39] W. Becker and D. B. Milošević, A gauge-covariant derivation of the strong-field approximation, Laser Phys. **19**, 1621 (2009).

[40] M. V. Frolov, N. L. Manakov, A. A. Minina, A. A. Silaev, N. V. Vvedenskii, M. Yu. Ivanov, and A. F. Starace, Analytic description of high-order harmonic generation in the adiabatic limit with application to an initial *s* state in an intense bicircular laser pulse, Phys. Rev. A **99**, 053403 (2019).

[41] N. L. Manakov, A. F. Starace, A. V. Flegel, and M. V. Frolov, Plateau effects in the spectra of electrons scattered from atoms in a strong laser field, Pis'ma Zh. Eksp. Teor. Fiz. **76**, 316 (2002) [JETP Lett. **76**, 258 (2002)].

[42] A. V. Flegel, M. V. Frolov, N. L. Manakov, A. F. Starace, and A. N. Zheltukhin, Analytic description of elastic electron-atom scattering in an elliptically polarized laser field, Phys. Rev. A **87**, 013404 (2013).

[43] E. A. Pronin, A. F. Starace, M. V. Frolov, and N. L. Manakov, Perturbation theory analysis of attosecond photoionization, Phys. Rev. A **80**, 063403 (2009).

[44] M. V. Frolov, N. L. Manakov, A. M. Popov, O. V. Tikhonova, E. A. Volkova, A. A. Silaev, N. V. Vvedenskii, and A. F. Starace, Analytic theory of high-order harmonic generation by an intense few-cycle laser pulse, Phys. Rev. A **85**, 033416 (2012).

[45] T. Morishita, A.-T. Le, Z. Chen, and C. D. Lin, Accurate Retrieval of Structural Information from Laser-Induced Photoelectron and High-Order Harmonic Spectra by Few-Cycle Laser Pulses, Phys. Rev. Lett. **100**, 013903 (2008).

[46] M. V. Frolov, D. V. Knyazeva, N. L. Manakov, J.-W. Geng, L.-Y. Peng, and A. F. Starace, Analytic model for the description of above-threshold ionization by an intense short laser pulse, Phys. Rev. A **89**, 063419 (2014).

[47] R. M. Potvliege and R. Shakeshaft, Multiphoton processes in an intense laser field: Harmonic generation and total ionization rates for atomic hydrogen, Phys. Rev. A **40**, 3061 (1989).

[48] N. L. Manakov, M. V. Frolov, B. Borca, and A. F. Starace, Multiphoton detachment of a negative ion by an elliptically polarized, monochromatic laser field, J. Phys. B: At. Mol. Opt. Phys. **36**, R49 (2003).

[49] M. V. Frolov, A. V. Flegel, N. L. Manakov, and A. F. Starace, Description of harmonic generation in terms of the complex quasienergy. I. General formulation, Phys. Rev. A **75**, 063407 (2007).

[50] A. N. Zheltukhin, A. V. Flegel, M. V. Frolov, N. L. Manakov, and A. F. Starace, Resonant electron-atom bremsstrahlung in an intense laser field, Phys. Rev. A **89**, 023407 (2014).

[51] A. N. Zheltukhin, A. V. Flegel, M. V. Frolov, N. L. Manakov, and A. F. Starace, Rescattering effects in laser-assisted electron–atom bremsstrahlung, J. Phys. B: At. Mol. Opt. Phys. **48**, 075202 (2015).

[52] A. Fleischer and N. Moiseyev, Amplification of high-order harmonics using weak perturbative high-frequency radiation, Phys. Rev. A **77**, 010102(R) (2008).

[53] A. Fleischer, Generation of higher-order harmonics upon the addition of high-frequency XUV radiation to IR radiation: Generalization of the three-step model, Phys. Rev. A **78**, 053413 (2008).

[54] T. S. Sarantseva, M. V. Frolov, N. L. Manakov, A. A. Silaev, N. V. Vvedenskii, and A. F. Starace, XUV-assisted high-order-harmonic-generation spectroscopy, Phys. Rev. A **98**, 063433 (2018).

[55] T. S. Sarantseva, M. V. Frolov, N. L. Manakov, A. A. Silaev, A. A. Romanov, N. V. Vvedenskii, and A. F. Starace, Attosecond-pulse metrology based on high-order harmonic generation, Phys. Rev. A **101**, 013402 (2020).

[56] T. S. Sarantseva, A. A. Silaev, A. A. Romanov, N. V. Vvedenskii, and M. V. Frolov, Time-frequency analysis of high harmonic generation using a probe XUV pulse, Opt. Express **29**, 1428 (2021).

[57] N. B. Delone, N. L. Manakov, and A. G. Fainshtein, Ionization of atoms by a low-frequency field and optical frequency field, Zh. Eksp. Teor. Fiz. **86**, 906 (1984) [J. Exp. Theor. Phys. **59**, 529 (1984)].

[58] G. Gademann, F. Kelkensberg, W. K. Siu, P. Johnsson, M. B. Gaarde, K. J. Schafer, and M. J. J. Vrakking, Attosecond control of electron–ion recollision in high harmonic generation, New J. Phys. **13**, 033002 (2011).

[59] M. B. Gaarde, K. J. Schafer, A. Heinrich, J. Biegert, and U. Keller, Large enhancement of macroscopic yield in attosecond pulse train–assisted harmonic generation, Phys. Rev. A **72**, 013411 (2005).

[60] J. Leeuwenburgh, B. Cooper, V. Averbukh, J. P. Marangos, and M. Ivanov, High-Order Harmonic Generation Spectroscopy of Correlation-Driven Electron Hole Dynamics, Phys. Rev. Lett. **111**, 123002 (2013).

[61] A. C. Brown and H. W. van der Hart, Extreme-Ultraviolet-Initated High-Order Harmonic Generation: Driving Inner-Valence Electrons Using Below-Threshold-Energy Extreme-Ultraviolet Light, Phys. Rev. Lett. **117**, 093201 (2016).

[62] J.-A. You, J. M. Dahlström, and N. Rohringer, Attosecond dynamics of light-induced resonant hole transfer in high-order-harmonic generation, Phys. Rev. A **95**, 023409 (2017).

[63] A. M. Perelomov and V. S. Popov, Ionization of atoms in an alternating electrical field. III, Zh. Eksp. Teor. Fiz. **52**, 514 (1967) [J. Exp. Theor. Phys. **25**, 336 (1967)].

[64] S. V. Popruzhenko, Invariant form of Coulomb corrections in the theory of nonlinear ionization of atoms by intense laser radiation, Zh. Eksp. Teor. Fiz. **145**, 664 (2014) [J. Exp. Theor. Phys. **118**, 580 (2014)].

[65] S. V. Popruzhenko, Keldysh theory of strong field ionization: History, applications, difficulties and perspectives, J. Phys. B: At. Mol. Opt. Phys. **47**, 204001 (2014).

[66] S. V. Popruzhenko, Coulomb phase in high harmonic generation, J. Phys. B: At. Mol. Opt. Phys. **51**, 144006 (2018).

[67] S. V. Popruzhenko, Quantum theory of strong-field frustrated tunneling, J. Phys. B: At. Mol. Opt. Phys. **51**, 014002 (2017).

[68] R. G. Newton, *Scattering Theory of Waves and Particles*, 2nd ed. (Springer Science & Business Media, New York, 2013), p. 745.

[69] R. Wong, *Asymptotic Approximations of Integrals* (SIAM, Philadelphia, 2001).